Laser driven fusion for energy with two beams

Laszlo P. Csernai, Univ. of Bergen, Norway

Wuhan University of Technology – Nov. 7, 2019


ENN新奥
新奥聚变技术研发中心
ENN Fusion Technology R&D Center

Indirectly Driven, ICF target for NIF at LLNL

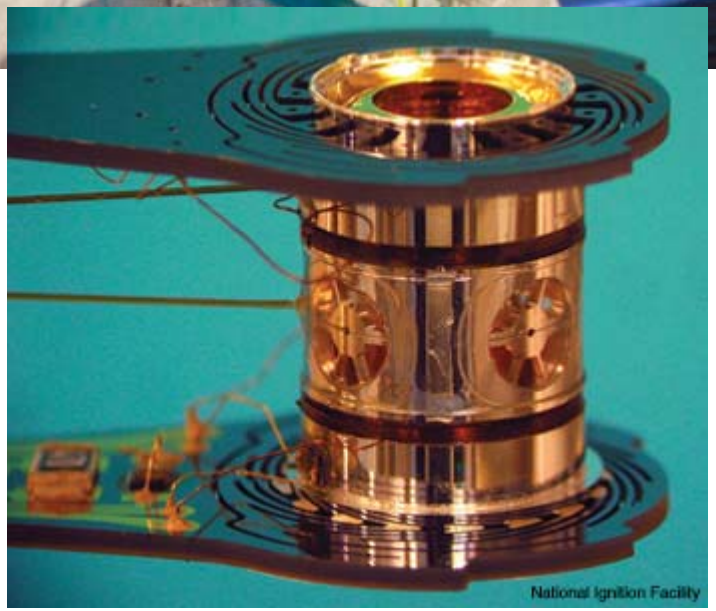

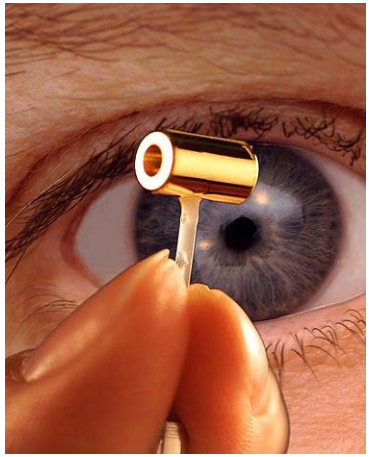

Indirectly Driven, ICF target for NIF

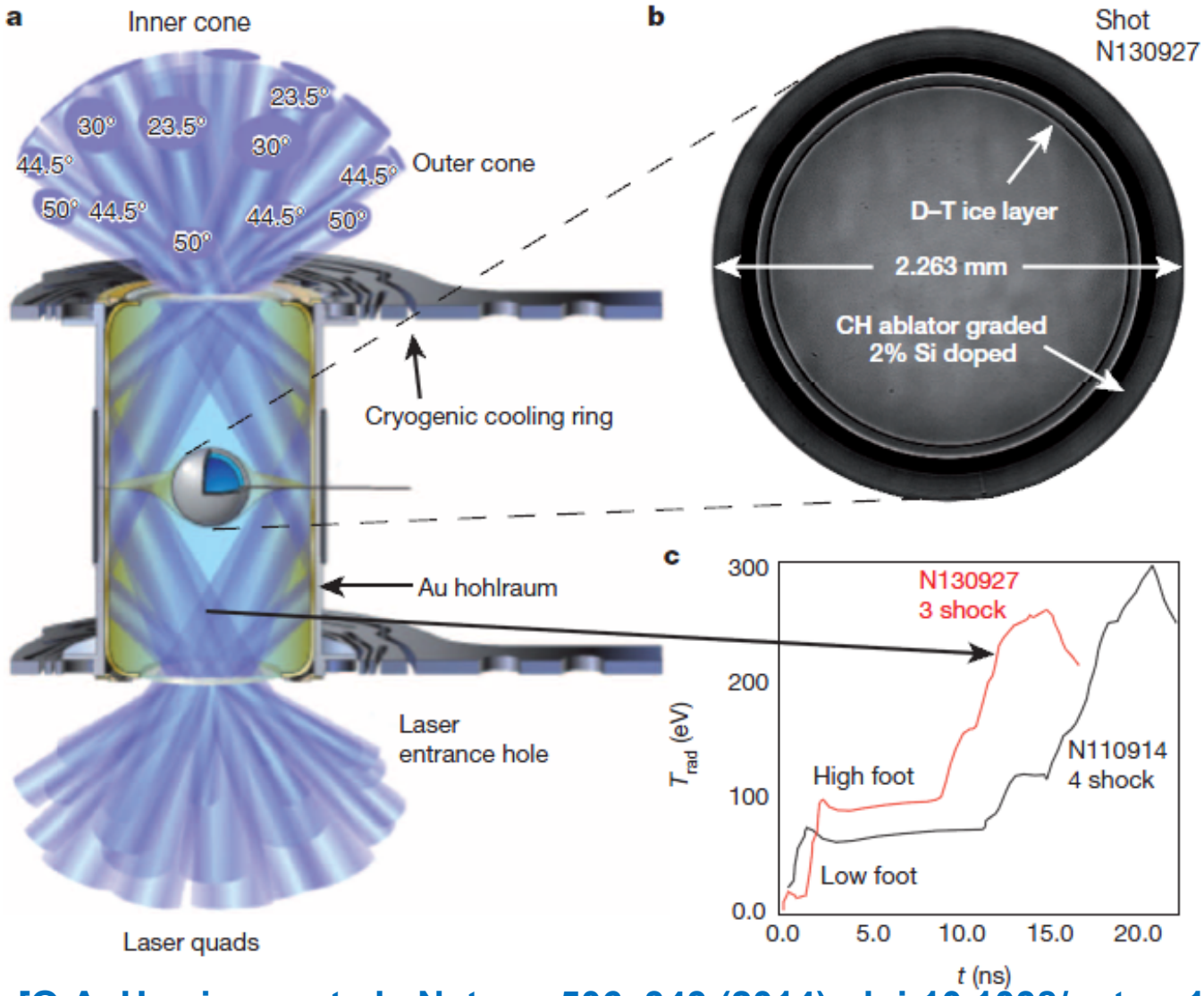

Time profile of the laser beam:

Initial pre-compression of ~ **10 ns**,
→ Stable compression

→ Then final "shocks" of ~ **15 ns** to ignite

[O.A. Hurricane et al., Nature, 506, 343 (2014), doi:10.1038/nature13008]

[Clark et al., Phys. Plasmas, **22**, 022703 (2015).]

Snapshots of 3D simulation
22.53ns: peak impl. Velocity
23.83ns: bang, max compr.
22.96ns: jet out, up left
Green surface: Ablator/DT-f.
Peaks: Ablator defects
Colours:
Left: fluid speed
Right: matter density

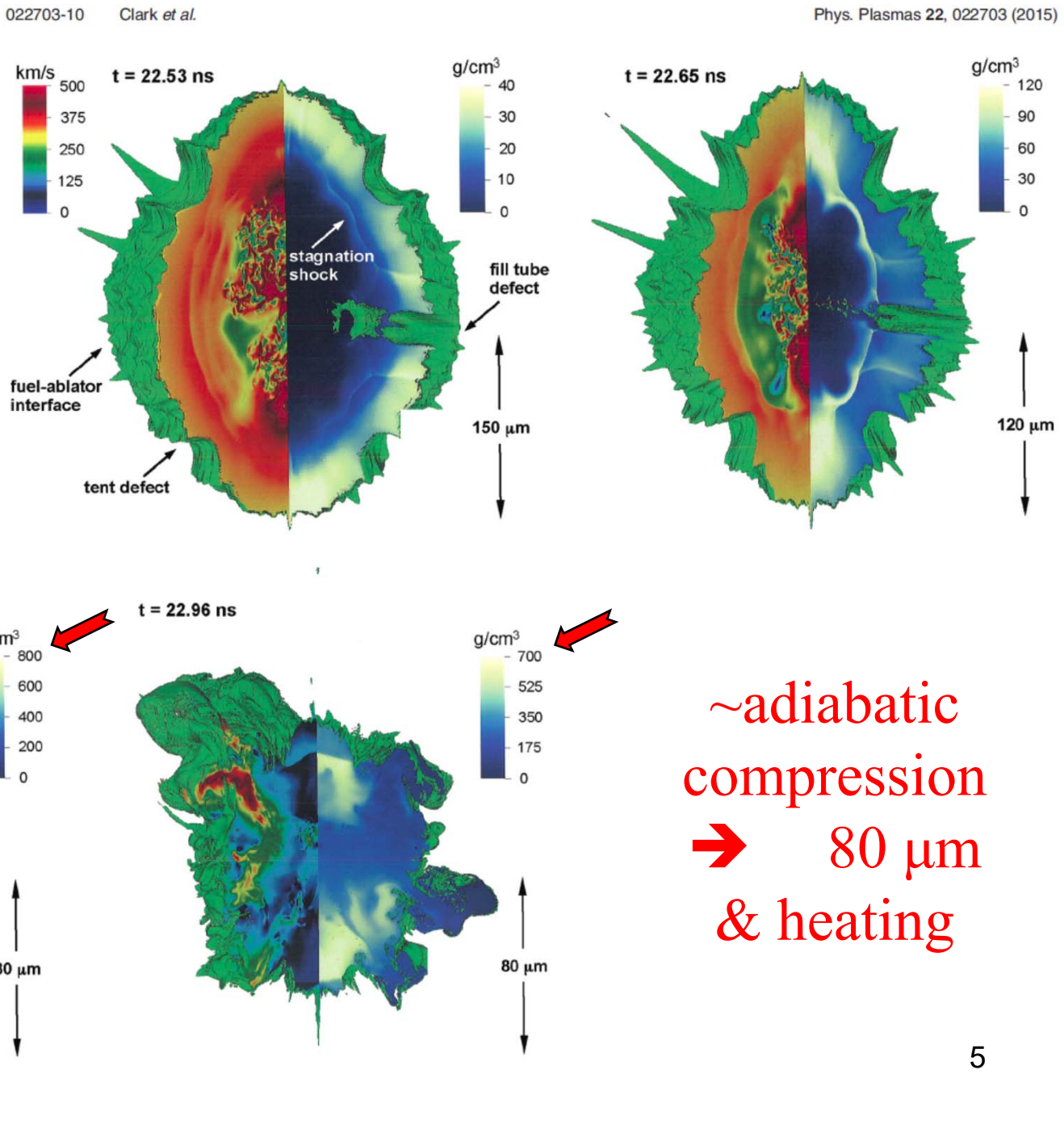

~adiabatic compression
➔ 80 µm
& heating

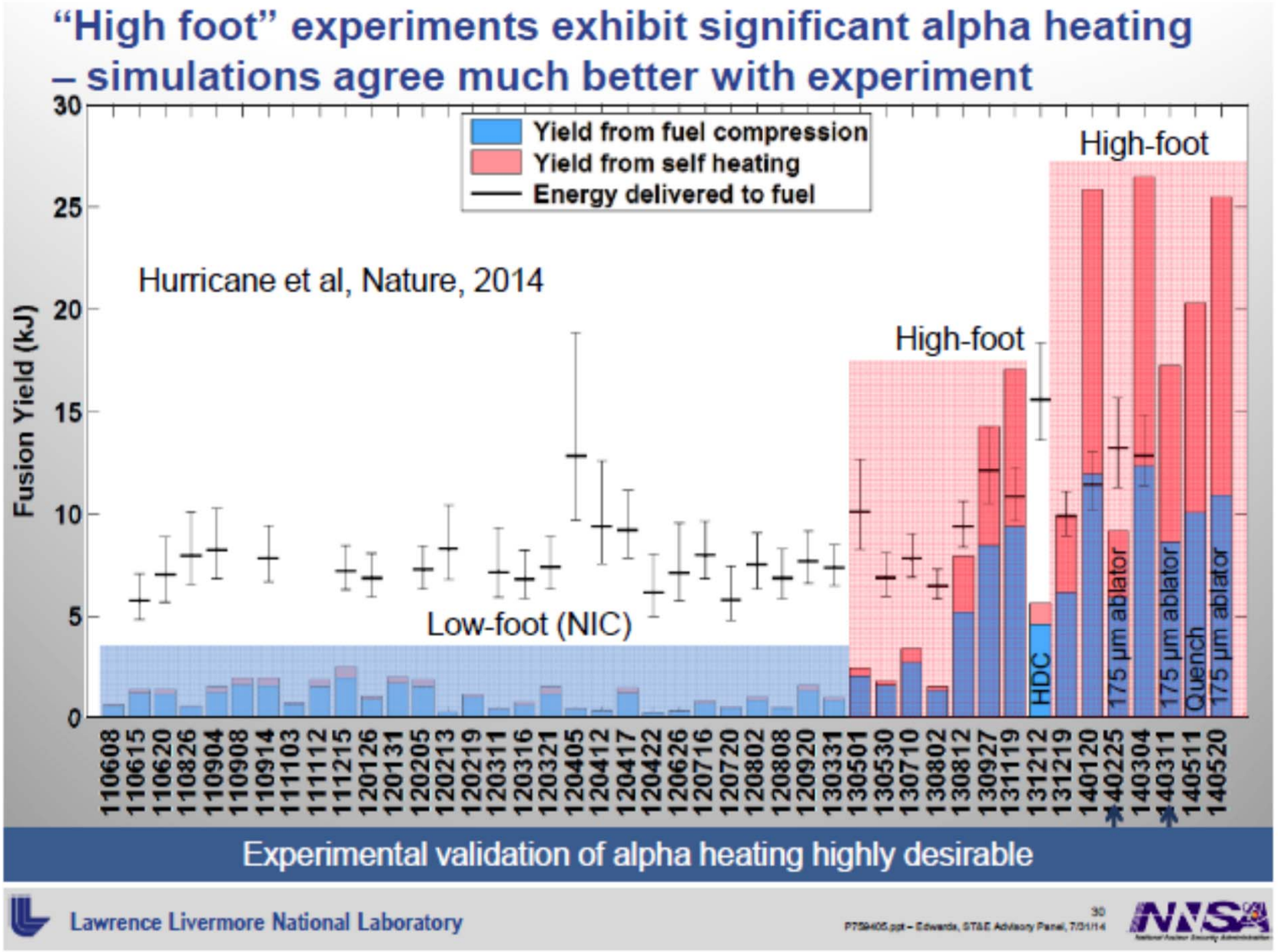

Phys. Rev. Lett. 120, 245003 – 14 June 2018:= Q' > 2

S. Le Pape et al., (LLNL - NIF)

Fusion Energy Output Greater than the Kinetic Energy of an Imploding Shell at the National Ignition Facility

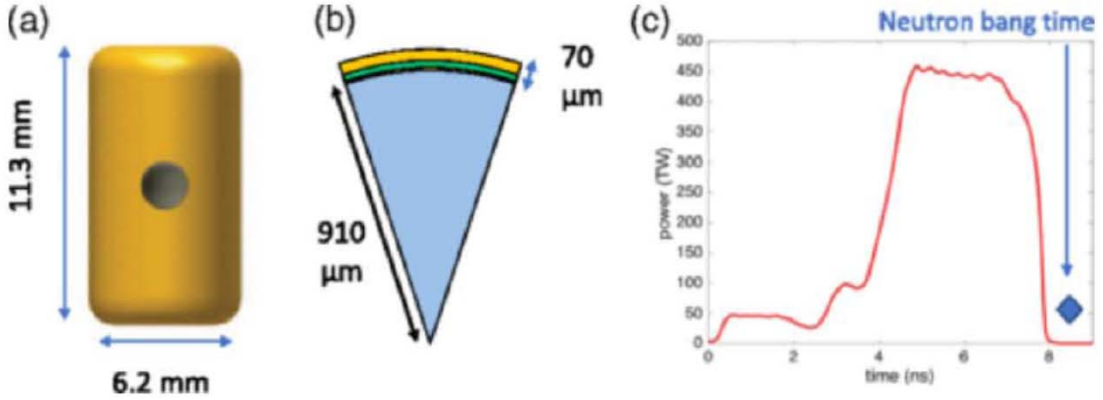

Depleted Uranium

Notice: The last energetic part of the pulse is less than **4ns**!
(It was ~ 15ns earlier.)

Figure 1

Target and laser specifications for shots N170601 and N170827. (a) 6.20 mm scale hohlraum (b) 70 μm thick HDC capsule used in the 6.20 mm scale hohlraum, green layer denotes the doped layer. This figure illustrates the doped layer of the HDC capsule. The doped HDC layer is 20 microns thick doped with 0.3% atomic percent of tungsten to shield the fuel from suprathermal x rays. This shielding is designed to reduce decompression of the inner capsule region and fuel and to improve the stability of the fuel-capsule interface. (c) Laser pulse.

published 14 June 2018

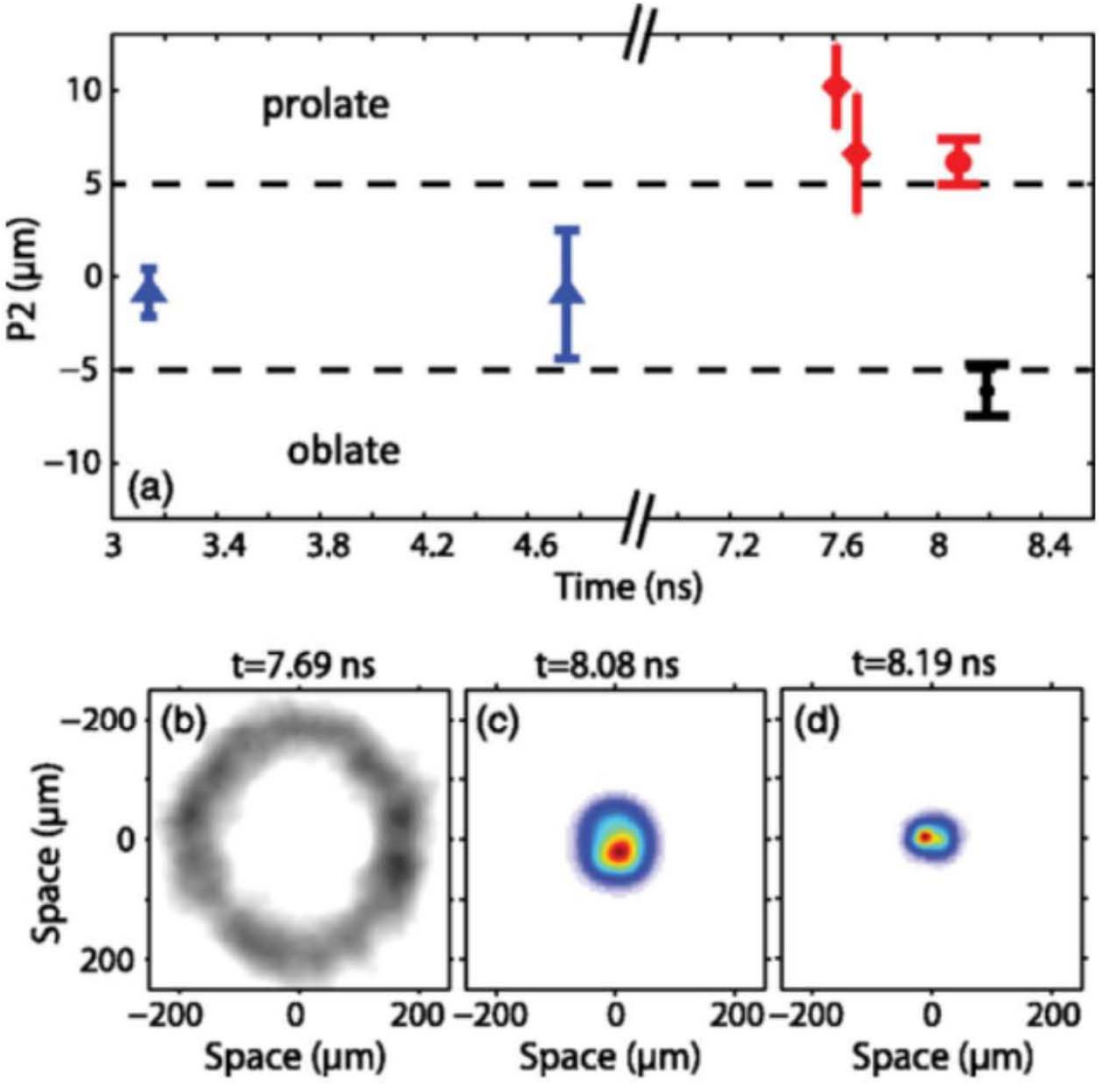

Figure 2

(a) History of the implosion symmetry for the doped HDC capsule measured at increasing convergence and time using a succession of experimental techniques. Blue points are keyhole data, red points are 2DconA data, black point is the DT cryogenic platform. The definition of $P2$ in microns as a measure of deviation from round is described in the text. (b) equatorial x-ray radiograph of the shell, (c) equatorial x-ray image of the hot spot at bang time (convergence 17) (d), equatorial x-ray image of the hot spot at bang time (convergence 25).

Notice: The ignition peak is now in the centre of the compressed target pellet!

80 μm - 2018

Approximate energy efficiency of diff. process steps of NIF:

Input energy of the laser (xenon lamps are powered by a capacitor bank)		422 MJ
Laser Infrared output (amplified IR light of the laser)		3.6 MJ
Laser UV output (about 50% is left after conversion to UV)	**2.1 MJ**	1.8 MJ
Laser energy absorbed by the hohlraum (theoretical prediction: about 85% is left after the X-ray conversion in the hohlraum)		<1.5 MJ
Laser energy absorbed by the outer layers of the DT target pellet (theoretical prediction: about 15% of the X-rays are absorbed by the outer layers of the target)		<220 kJ
Actual energy absorbed by the DT target pellet (based on report that more energy for this shot was released than UV-energy that is absorbed in the DT-target).		<14 kJ

Energy out

Energy released by fusion reactions (fraction 3.3×10^{-5} of input energy of the laser)	**14 kJ**	~14 kJ

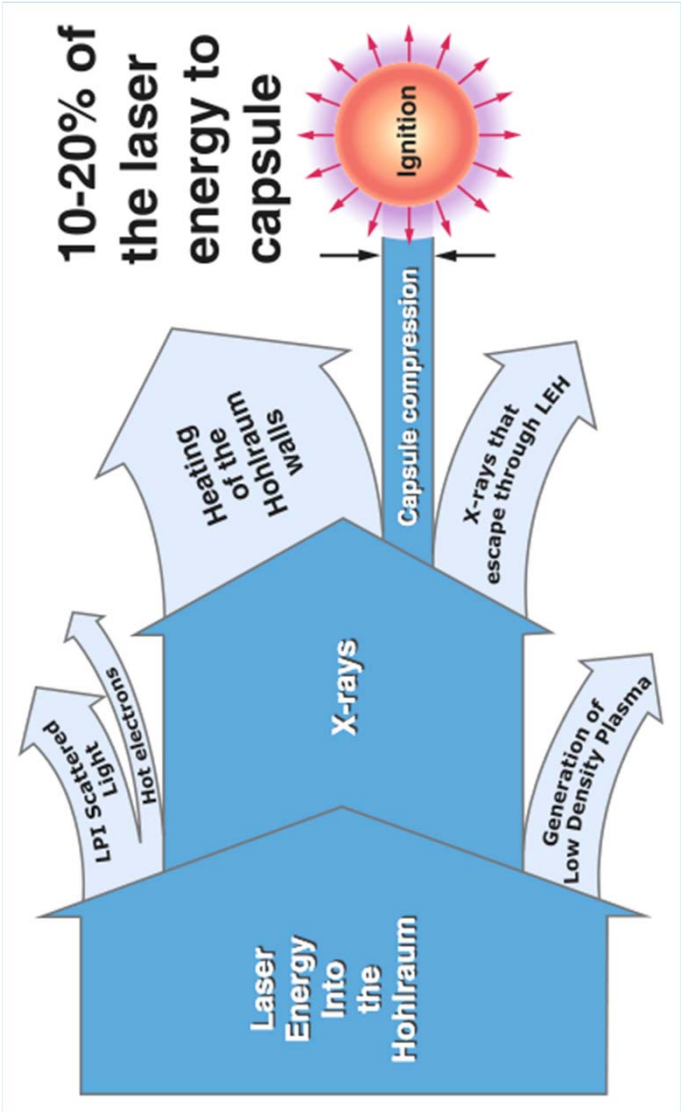

2014:= 0.003318% !

2018:= fusion energy of 54 kJ.

Burning of Quark Gluon Plasma in Relativistic, Radiation Dominated Systems according to Relativistic Fluid Dynamics

-

Applications to Pellet Fusion

Classical Fluid Dynamics (CFD) does assumes that all dynamical processes, including shocks and detonations, are having speeds slower than the speed of light, c.

Initial Relativistic FD (RFD) maintained this assumption based on the requirement of causality [A.Taub, 1948].→ Engineering books keep this assumption even today!

Relativistic Heavy Ion Physics proved the opposite!

[A.H. Taub (1948)]

PHYSICAL REVIEW VOLUME 74, NUMBER 3 AUGUST 1, 1948

Relativistic Rankine-Hugoniot Equations

A. H. TAUB
*University of Illinois, Urbana, Illinois and Institute for Advanced Study, Princeton University, Princeton, New Jersey**

Next we suppose that the three-dimensional volume is a shell of thickness ϵ enclosing a surface of discontinuity $\sum$ whose three-dimensional normal vector is Λ_i. If we choose our coordinate system so that the discontinuity is at rest, then since

$$\lambda_\alpha\lambda^\alpha=1, \quad \sum_{i=1}^{3}\Lambda_i^2=1,$$

we have

$$\lambda_i=\Lambda_i \quad \text{and} \quad \lambda_4=0.$$

Hence Eqs. (7.1) and (7.2) become, as ϵ goes to zero,

$$[\rho^0 u^i\Lambda_i]=0, \tag{7.3}$$

$$[T^{\alpha i}\Lambda_i]=0, \tag{7.4}$$

where

$$[f]=f_+-f_-$$

Taub assumed that (physically) only slow space-like shocks or discontinuities may occur (with space-like normal, $\lambda_4=0$).

This was then taken as standard, since then (e.g. LL 1954-)

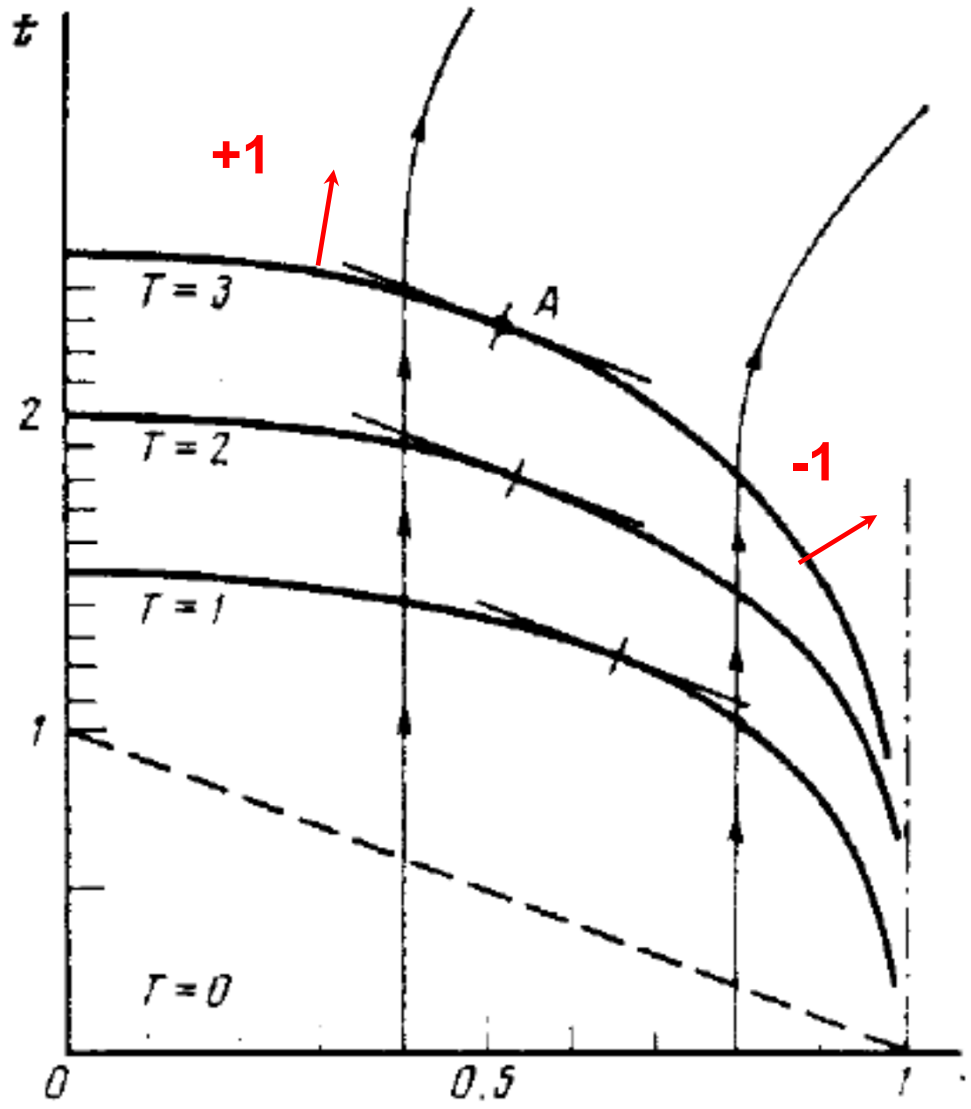

[L. P. Csernai, Zh. Eksp. Teor. Fiz. 92, 379-386 (**1987**) & Sov. Phys. JETP 65, 216-220 (1987)]

corrected the work of [**A. Taub**, Phys. Rev. 74, 328 (**1948**)]

$$\lambda_\alpha \, \lambda^\alpha = \pm 1$$

Л. П. Чернаи

ДЕТОНАЦИЯ НА ВРЕМЕНИПОДОБНОМ ФРОНТЕ ДЛЯ РЕЛЯТИВИСТСКИХ СИСТЕМ

Журнал экспериментальной и теоретической физики 1987

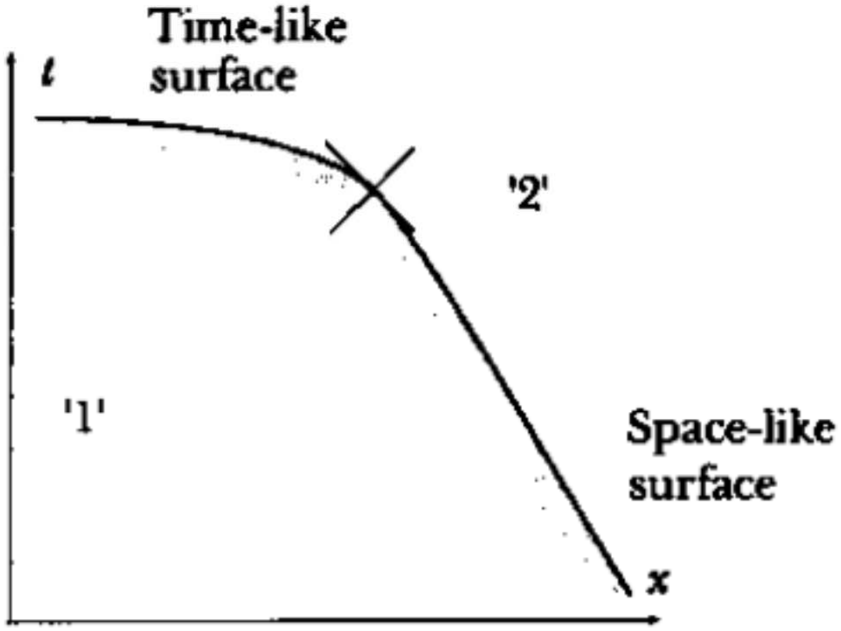

[L.P. Csernai:
Introduction to Relativistic Heavy Ion Collisions,
(**1994**, John Wiley & Sons, Cichester, England)]

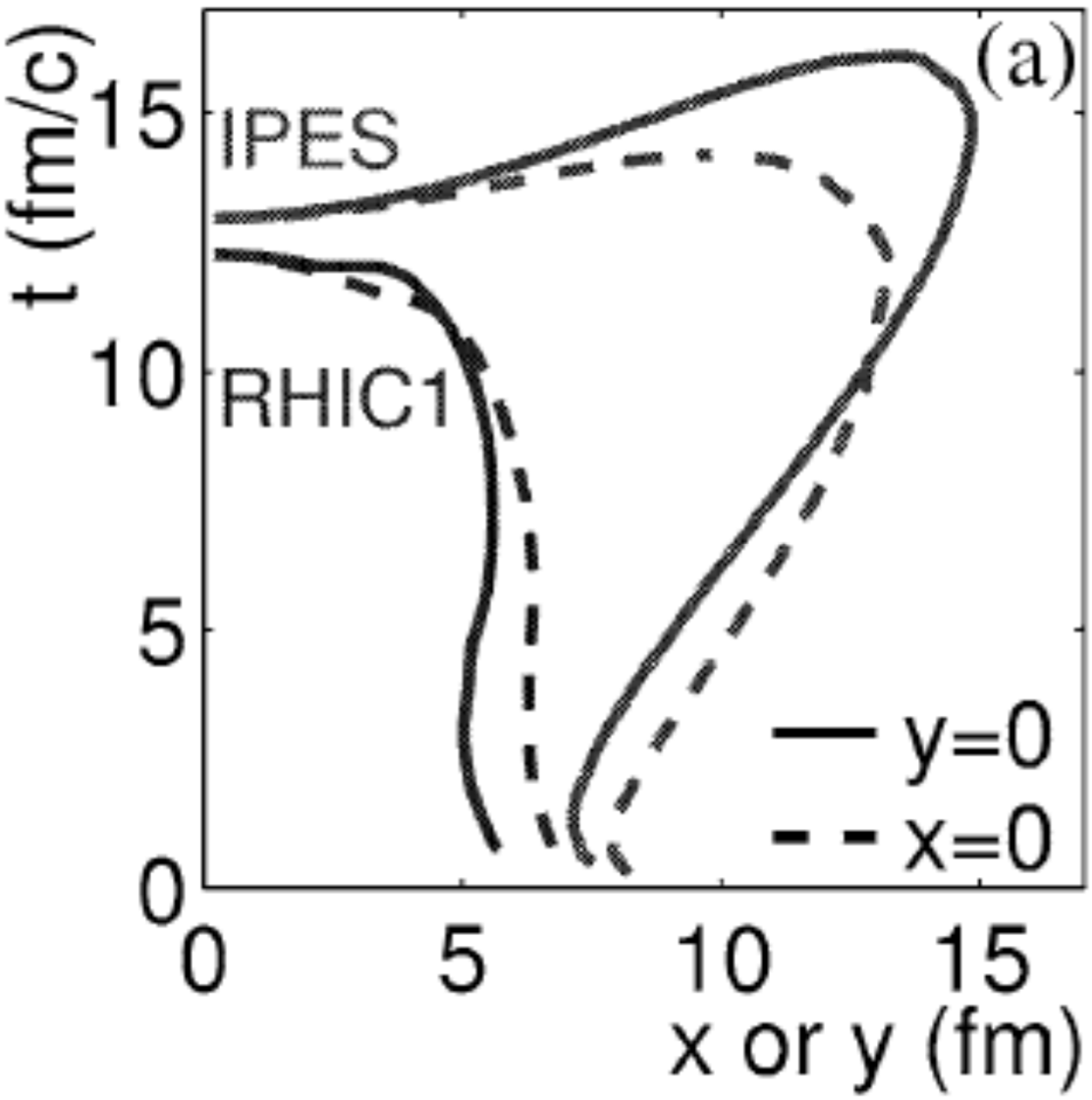

Discovery of QGP:
2000 CERN
2001 BNL

[U.W. Heinz and P.F. Kolb, Phys. Lett. B 542, 216 (2002)]

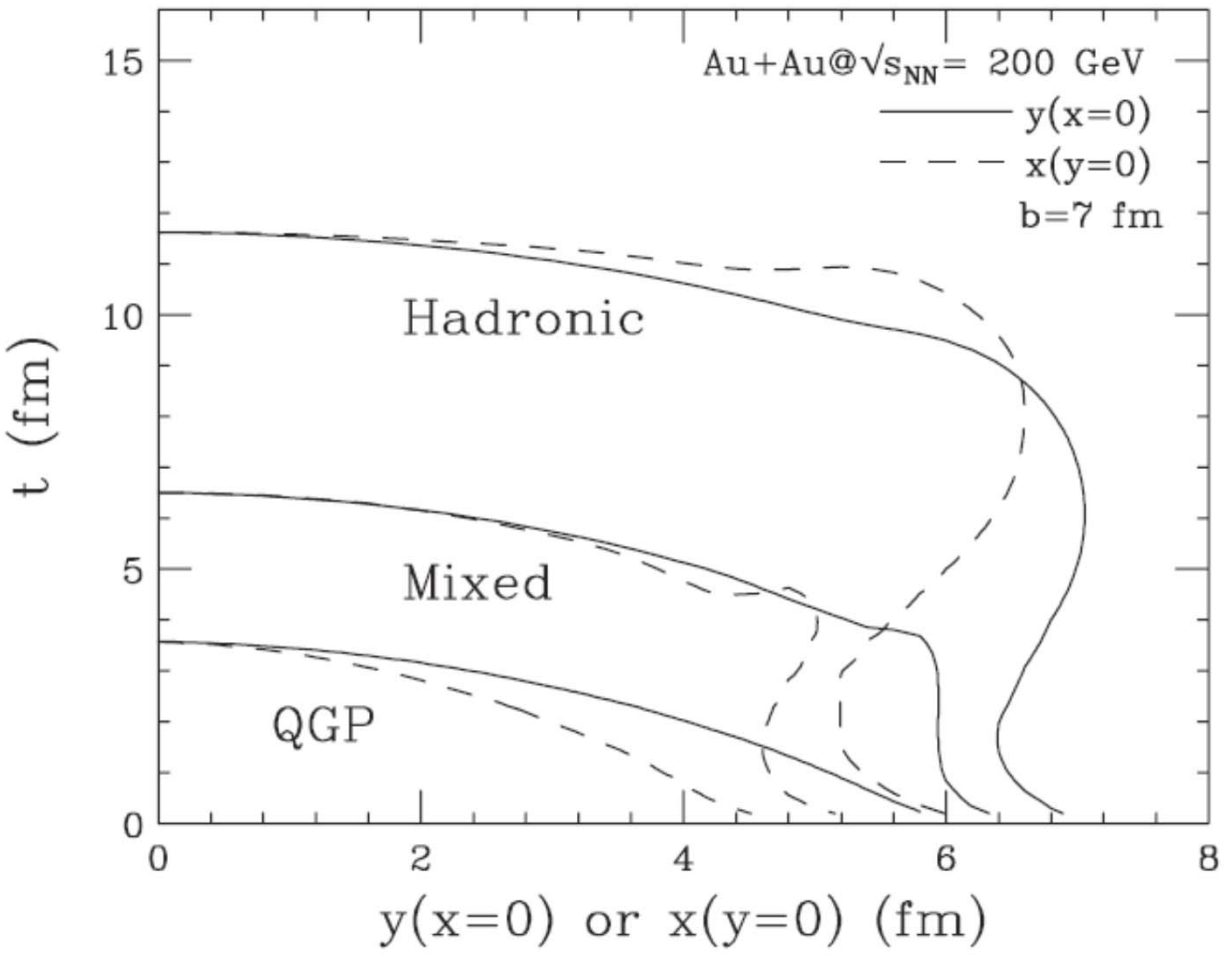

[R. Chatterjee, et al., Phys. Rev. Lett. 96, 202302 (2006)]

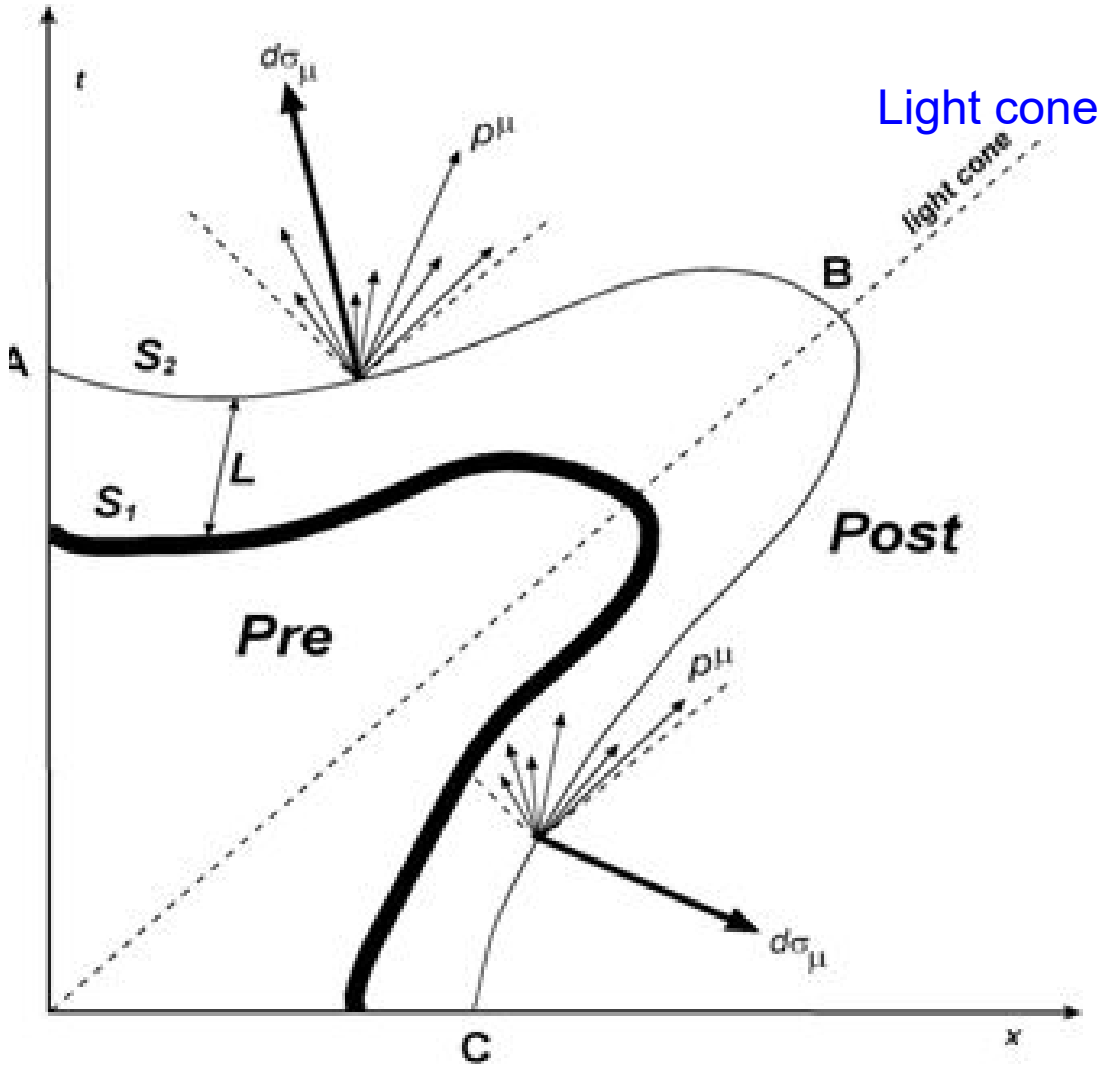

Light cone

[E. Molnar, et al., J. Phys. G 34 (2007) 1901]

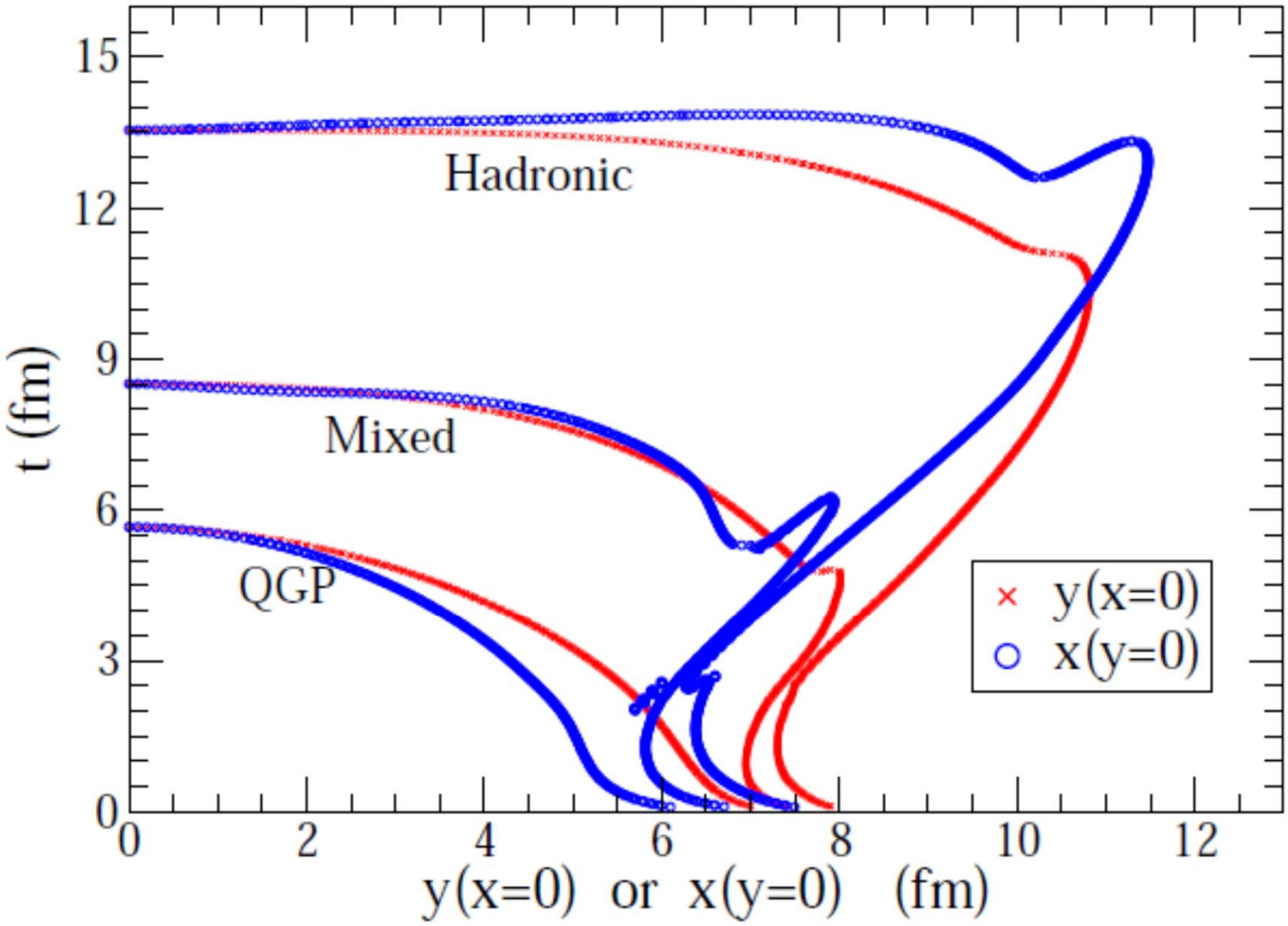

[E. Frodemann, et al., J.Phys. G 34, 2249-2254 (2007)]

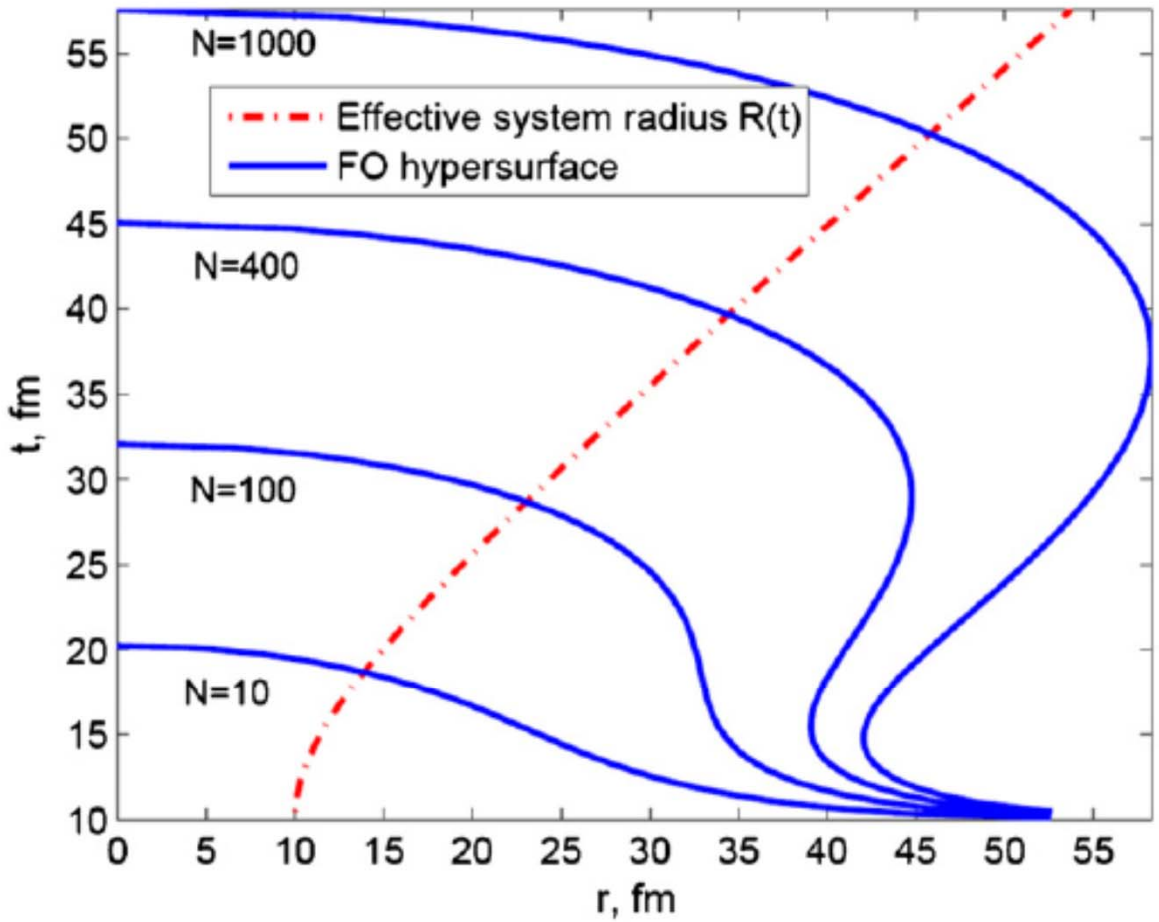

Figure 4. Freeze-out surfaces calculated from the Bondorf condition (see the text) for various particle numbers *N*.

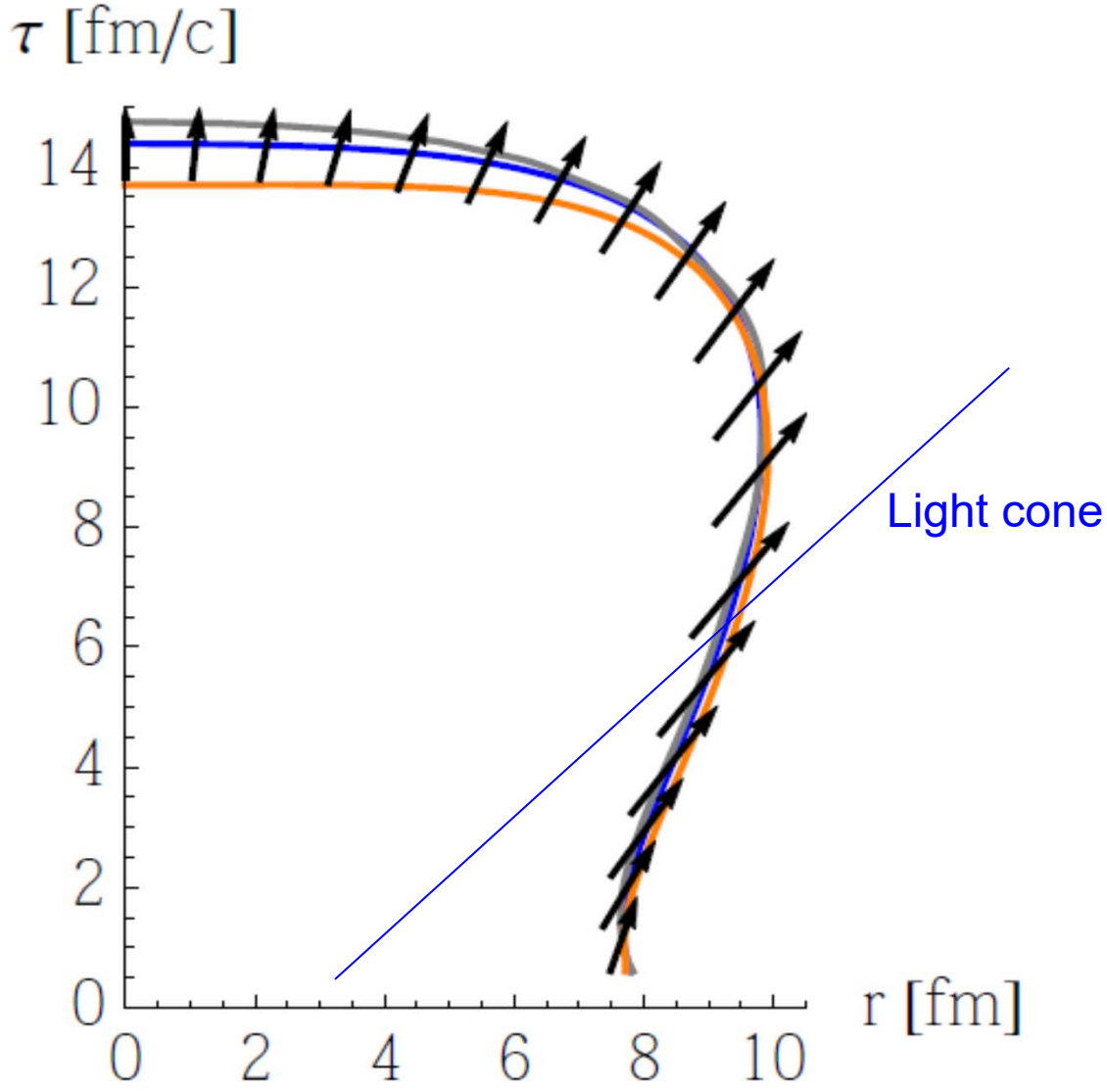

[Stefan Floerchinger, and Urs Achim Wiedemann, Phys. Rev. C 89, 034914 (2014)]

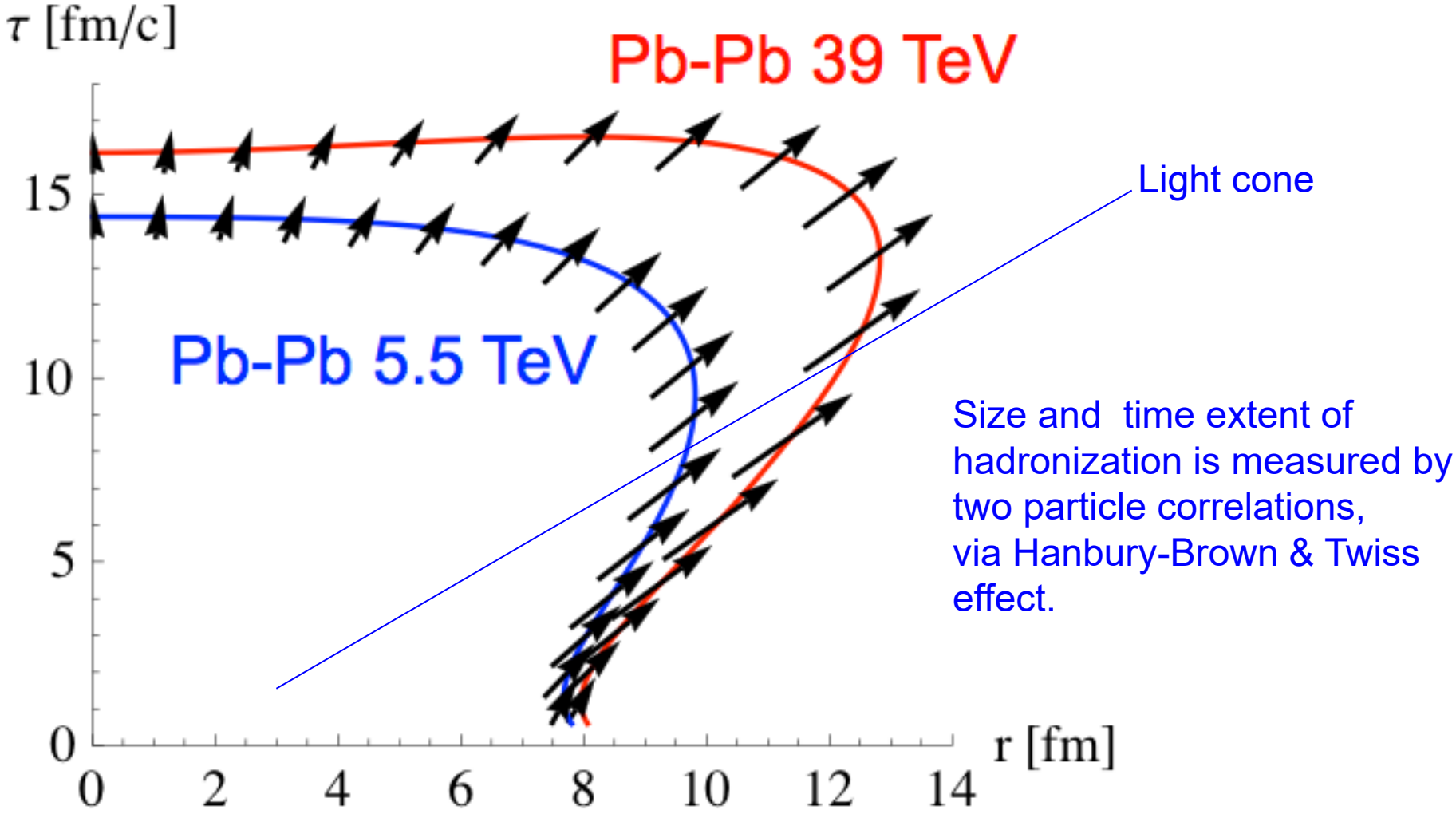

[N. Armesto, et al., Nucl.Phys. A931 (2014) 1163]

Applications to Pellet Fusion (I-st)

Relativistic Heavy Ion Physics proves that simultaneous ignition and burning is possible, both theoretically and experimentally (two particle corr.) !

Up to now all theoretical studies of Internal Confinement fusion are based on Classical Fluid Dynamics (CFD)
[HYDRA, LASNEX]

Still the aim is to

- achieve Volume Ignition
- achieve Rapid Ignition
- but within CFD ?! →

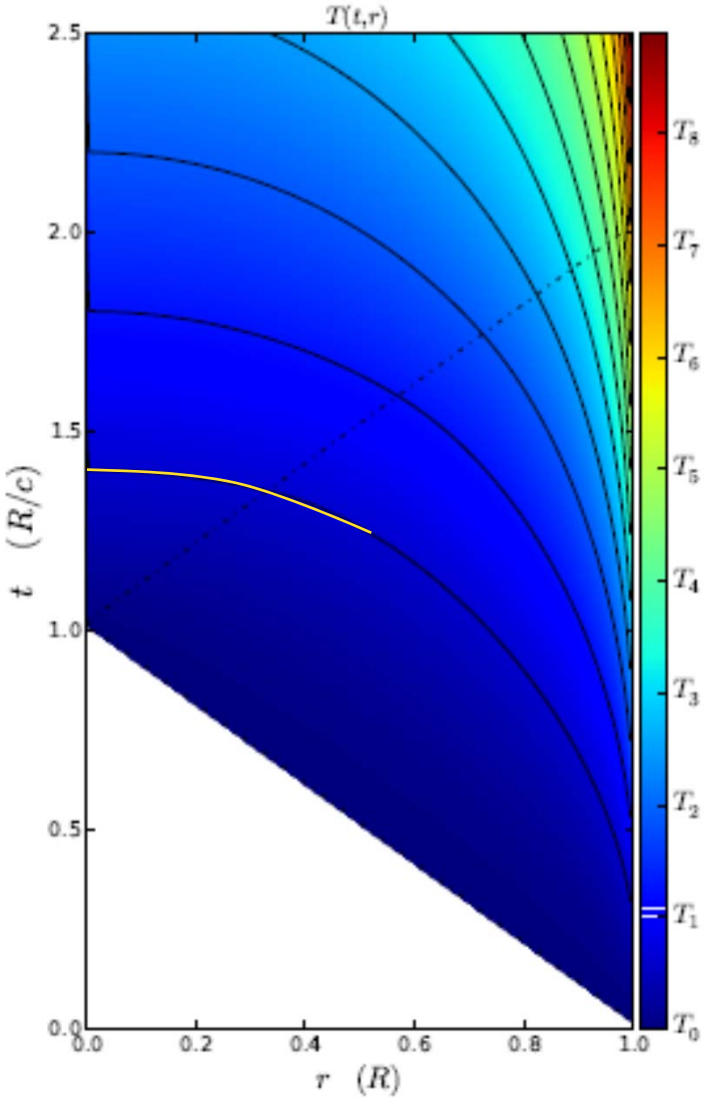

[L.P. Csernai & D.D. Strottman,
Laser and Particle Beams 33, 279 (2015).]

Fusion reaction:

D + T ➔ n(14.1 MeV) + 4He (3.5 MeV)

Constant absorptivity,
Spherical irradiation
Ignition temperature = T1 ➔

Simultaneous, volume ignition up to 0.5 R (i.e. **12%** of the volume).

Not too good, but better than:

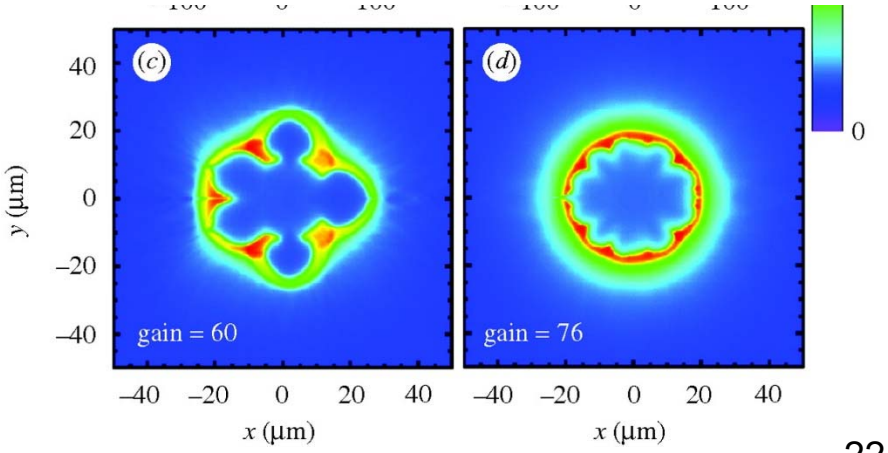

Can we achieve larger volume ignition (II-nd)

Two ideas are combined by
L.P. Csernai, N. Kroo, I. Papp **[Patent # P1700278/3](*)**

- **Heat the system uniformly by radiation with RFD**
- **Achieve uniform heating by Nano-Technology**

Mechanical compression and adiabatic heating should be reduced, because it is slow and leads to Rayleigh-Taylor instabilities. Similarly outside ablator surface should be reduced also.

Uniform, **4π radiation** should heat the target to ignition within the light penetration time (i.e. ~ 10-20 ps). This follows from RFD!

[L.P. Csernai, N. Kroo, I. Papp, *Laser and Particle Beams,* LPB, 36(2), (2018) 171-178. .
https://doi.org/10.1017/S0263034618000149]

LPB, 36(2), (2018) 171-178.
Laser and Particle Beams

cambridge.org/lpb

Radiation dominated implosion with nano-plasmonics

L.P. Csernai[1], N. Kroo[2,3] and I. Papp[4]

[1]Department of Physics and Technology, University of Bergen, Bergen, Norway; [2]Hungarian Academy of Sciences, Budapest, Hungary; [3]Wigner Research Centre for Physics, Budapest, Hungary and [4]Department of Physics, Babes-Bolyai University, Cluj, Romania

Research Article

Cite this article: Csernai LP, Kroo N, Papp I (2018). Radiation dominated implosion with nano-plasmonics. *Laser and Particle Beams* 1–8. https://doi.org/10.1017/S0263034618000149

Received: 28 November 2017
Revised: 14 March 2018
Accepted: 3 April 2018

Key words:
Inertial confinement fusion; nano-shells; relativistic fluid dynamics; time-like detonation

Author for correspondence:
L.P. Csernai, Department of Physics and Technology, University of Bergen, Bergen, Norway. E-mail: Laszlo.Csernai@uib.no

Abstract

Inertial Confinement Fusion is a promising option to provide massive, clean, and affordable energy for mankind in the future. The present status of research and development is hindered by hydrodynamical instabilities occurring at the intense compression of the target fuel by energetic laser beams. A recent patent combines advances in two fields: Detonations in relativistic fluid dynamics (RFD) and radiative energy deposition by plasmonic nano-shells. The initial compression of the target pellet can be decreased, not to reach the Rayleigh–Taylor or other instabilities, and rapid volume ignition can be achieved by a final and more energetic laser pulse, which can be as short as the penetration time of the light across the pellet. The reflectivity of the target can be made negligible as in the present direct drive and indirect drive experiments, and the absorptivity can be increased by one or two orders of magnitude by plasmonic nano-shells embedded in the target fuel. Thus, higher ignition temperature and radiation dominated dynamics can be achieved with the limited initial compression. Here, we propose that a short final light pulse can heat the target so that most of the interior will reach the ignition temperature simultaneously based on the results of RFD. This makes the development of any kind of instability impossible, which would prevent complete ignition of the target.

… and 35th Hirschegg Int. Workshop on High Energy Density Physics, Jan. 25-30, 2015

Golden Nano-Shells – Resonant Light Absorption

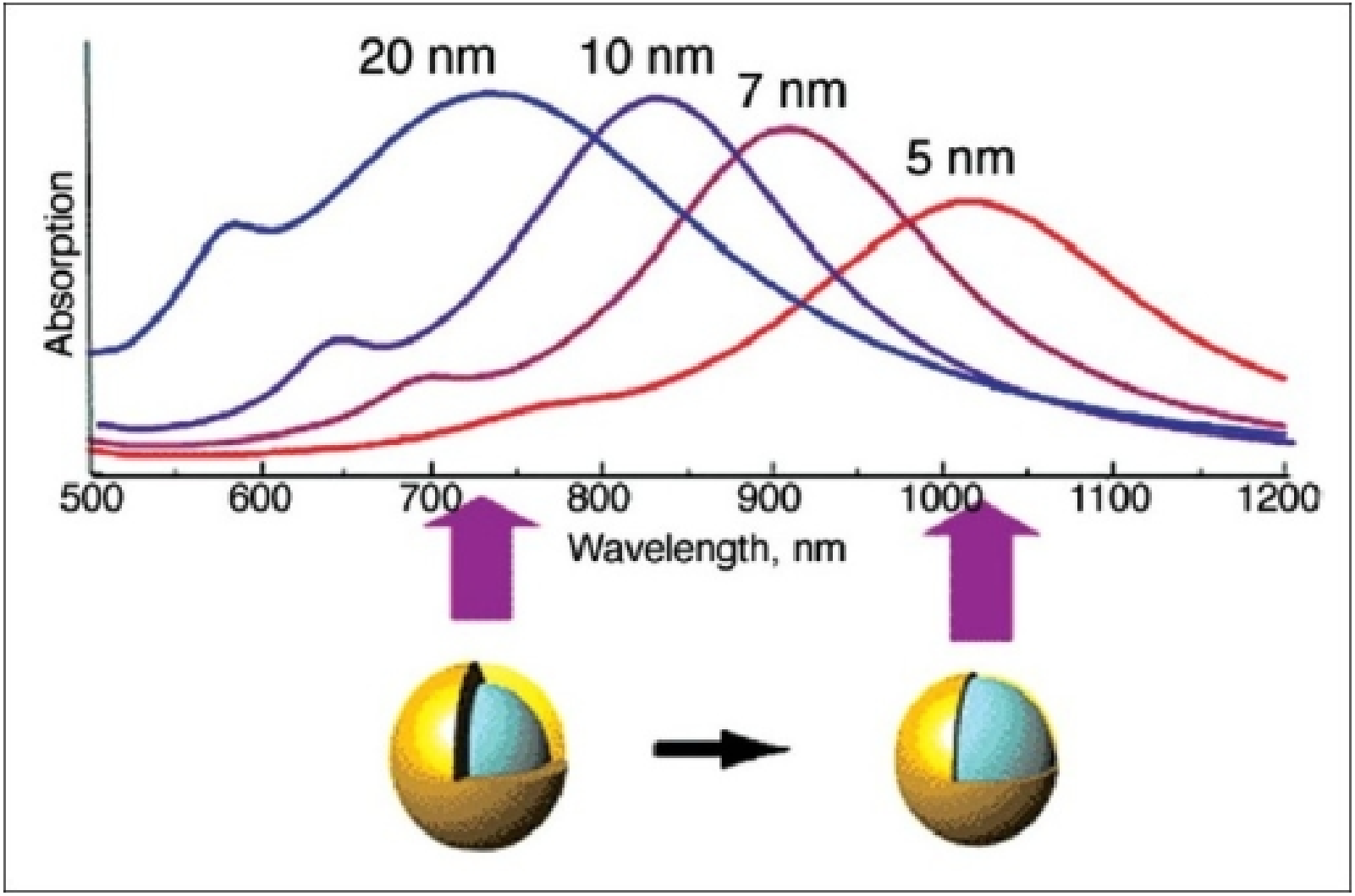

Metal nanoparticles (MNP) and their optical properties

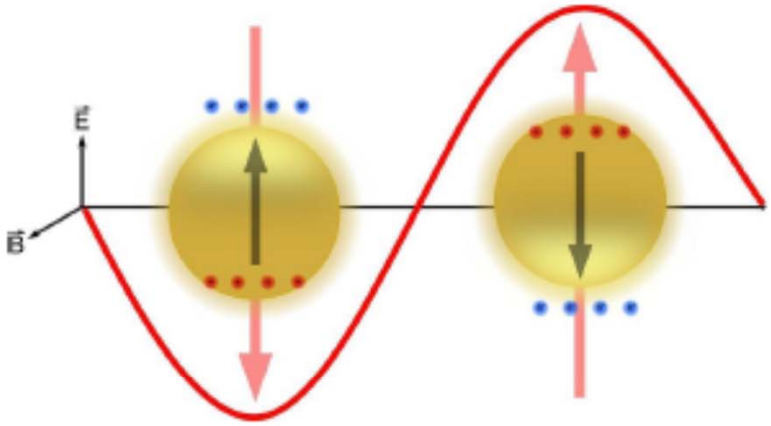

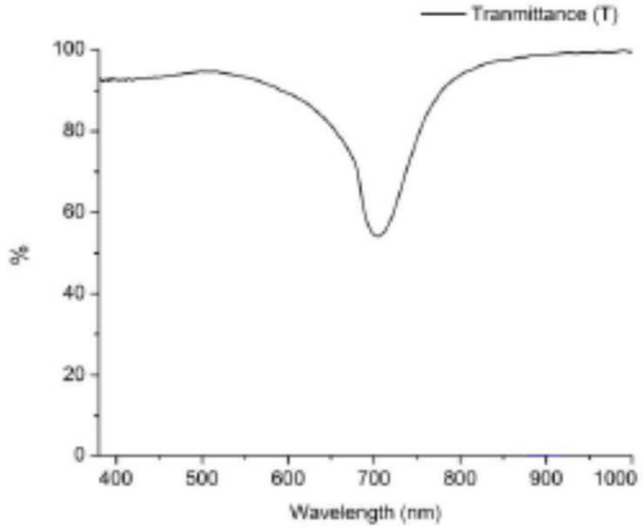

[Martin Greve, IFT Seminar, Fall (2017) for PV Solar panels]

Localized Surface Plasmon Resonance (LSPR)!

Omnidirectional TV antenna

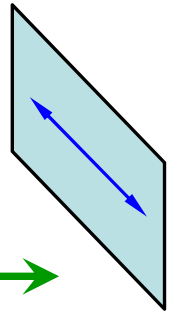

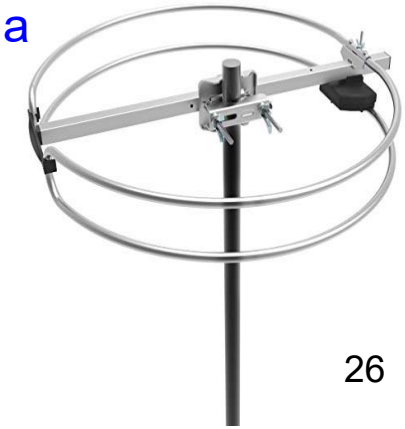

Laser and Particle Beams

cambridge.org/lpb

Radiation dominated implosion with nano-plasmonics

L.P. Csernai[1], N. Kroo[2,3] and I. Papp[4]

doi.org/10.1017/S0263034618000149 LPB, 36(2), (2018) 171-178.

Variation of absorptivity by Nanotechnology

Doping INF pellets with golden nano-shells enables us to achieve the desired variable absorptivity (Tanabe, 2016).

$$\alpha_k = \alpha_{k0} + \alpha_{ns} \ , \tag{12}$$

where the absorptivity of nano-shells, α_{ns}, is

$$\alpha_{ns} = \rho G Q_{abs}. \tag{13}$$

For a nano-shell of $R = 30$ nm the additional contribution would be $\rho G Q_{abs} = \rho Q_{abs}$ 0.283 cm^2. Consequently, for a typical nano-shell density (James *et al.*, 2007) of $\rho = 10^{11}$/cm^3 and a $Q_{abs} \approx 10$, we can reach an additional absorptivity of

$$\alpha_{ns} = 28.3 \text{ cm}^{-1}. \tag{14}$$

L.P. Csernai, N. Kroo, I. Papp **[Patent # P1700278/3](*)**

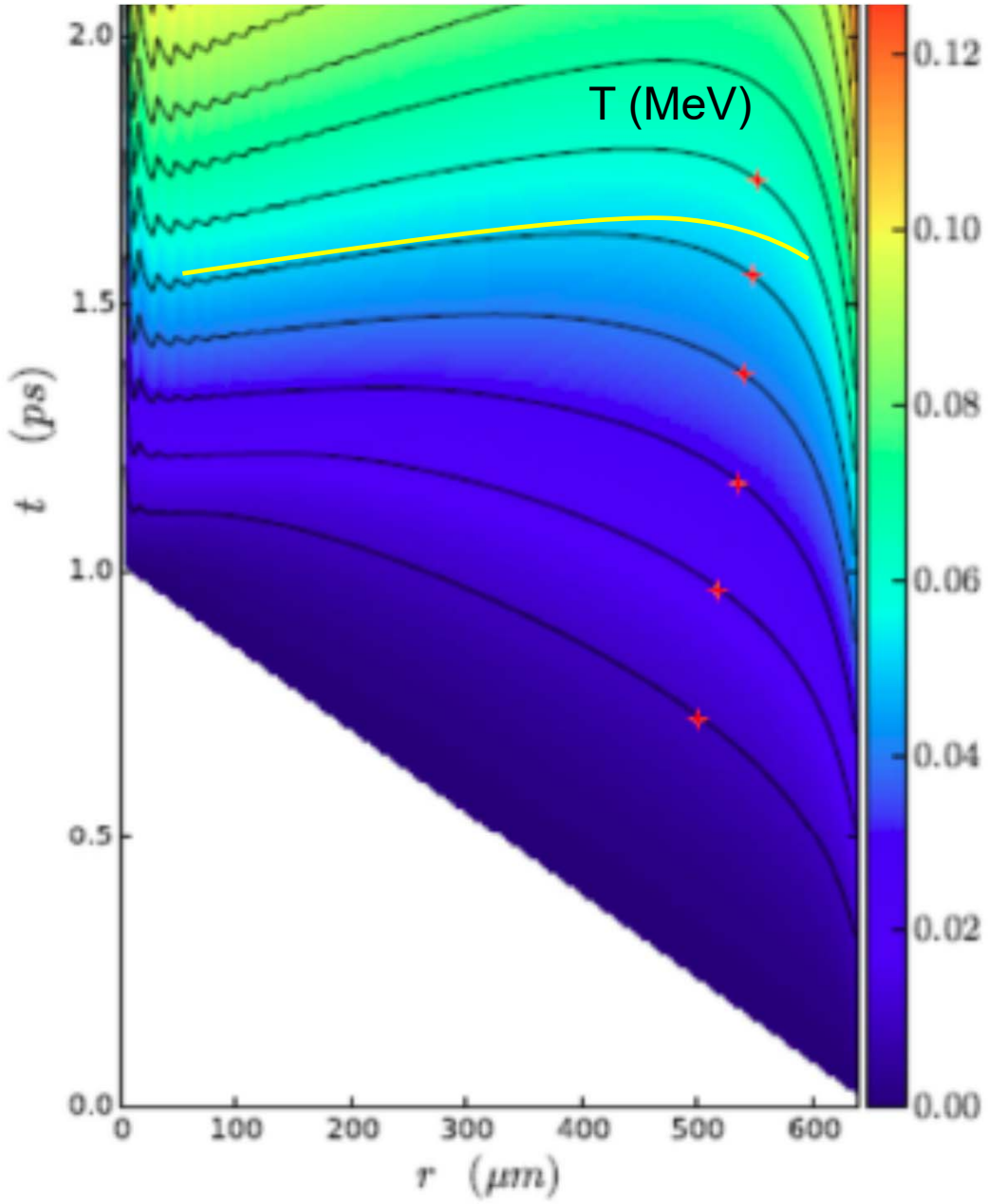

The absorption coefficient is **linearly** changing with the radius: In the center,

$r = 0$, $\alpha_K = 30\ cm^{-1}$ while at the outside edge $\alpha_K = 8\ cm^{-1}$.

The temperature is measured in units of $T_1 = 272$ keV, and $T_n = n\ T_1$.

Simultaneous, volume ignition is up to 0.9 R, so **73% of the fuel target!**

Problem:

Not easy to realize, 4π irradiation geometry ➔ **80-192 laser beams**

In the earlier estimates we did establish that:
- The principle of simultaneous volume ignition is theoretically possible with nano-spheres or nano-rods (i.e. nano-antennas).
- We **did not** estimate the necessary laser energy need, and assuming extremely large laser input energy we neglected the losses.

- However the basic principle, the **simultaneous all volume ignition** can be achieved in 3D, 2D and 1D geometry also !!!
  (Einstein's synchronization of watches.)

- We did calculate the realistic energy balance

- ➔ So, we repeated realistic estimates in 1D with a flat (coin or rod like) target.

Thick Coin like target - New Developments

L.P. Csernai, N. Kroo, I. Papp

X

Thickness of the target is: h

h depends on pulse energy, ignition energy, target mass, …

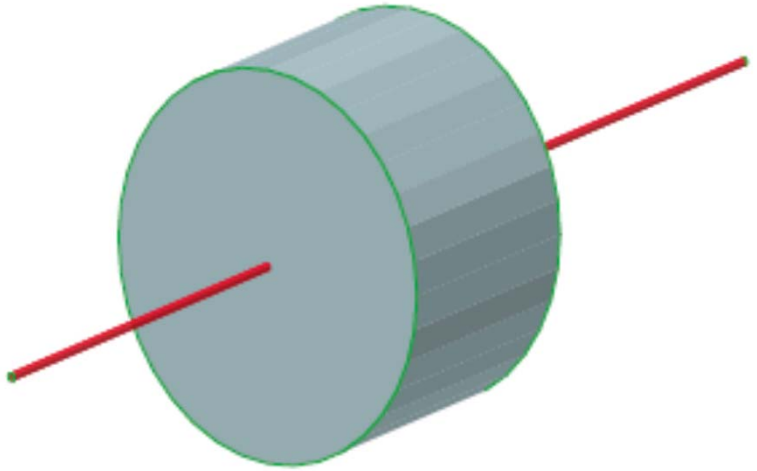

Figure 1: (color online) The target still should be compact to minimize the surface effects. The irradiation is performed along the $x-$axis from both sides towards the target. The laser beam should be uniform hitting the whole face of the coin shaped target.

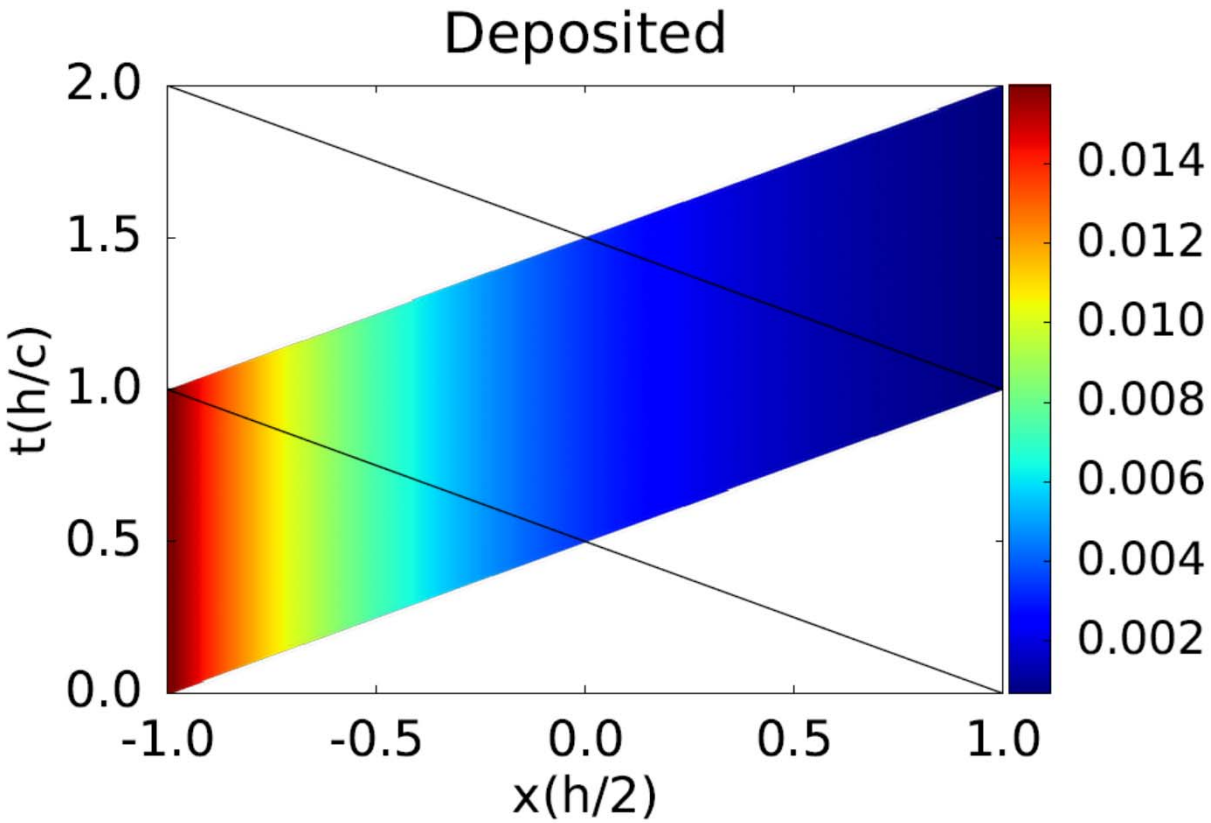

Without nano antennas

The deposited energy from laser irradiation from one side only. The absorption is constant, this leads to an exponentially decreasing energy deposition, and only a negligibly small energy reaches the opposite end of the target.

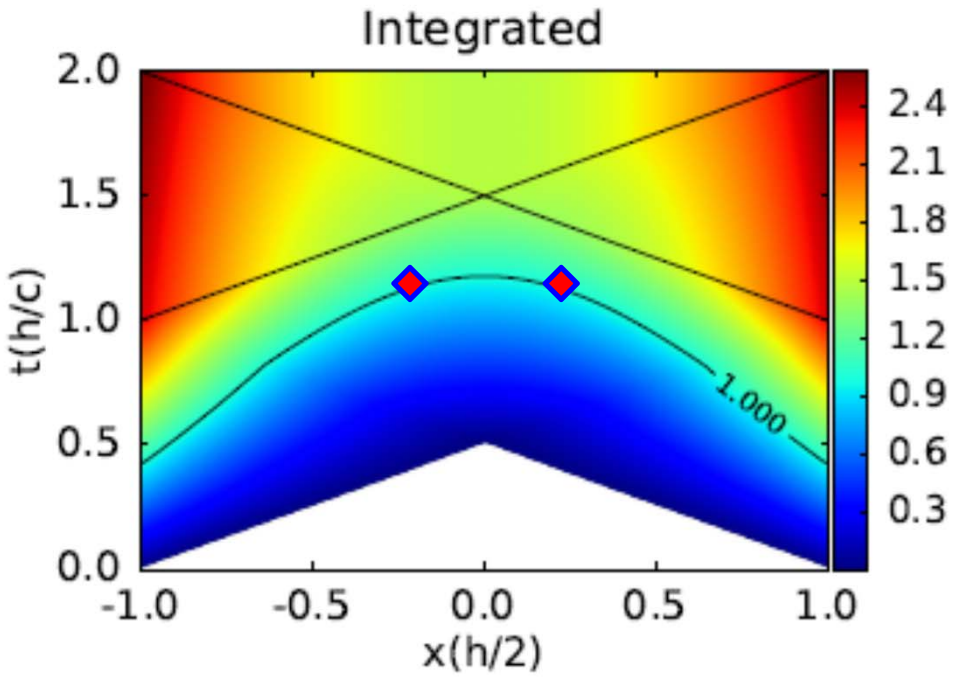

Figure 4: (color online) Integrated energy up to a given time in the space-time across the depth, h, of the flat target. The color code indicates the temperature, T, reached in a given space-time point, in units of the critical temperature, (T_c). The contour line $T = 1$, indicates the critical temperature, T_c, where the phase transition or the ignition in the target is reached. This contour line, compared to the one in Fig. 3, is never constant in time, indicating no simultaneous whole volume transition or ignition. The time-like (causally unconnected) part of the transition takes place only in the central $\sim$ 15% of the target volume. The two straight lines indicate the light-cones originating at the outside edges of the target at the ending of the irradiation pulse.

Without nano antennas

Irradiation from both sides.

Exponential decrease of deposited energy. Due to the already deposited energy, less energy reaches the middle ➔

The front and back surface is heated up but the middle is not!

Pulse length is: $t_P = h/c$

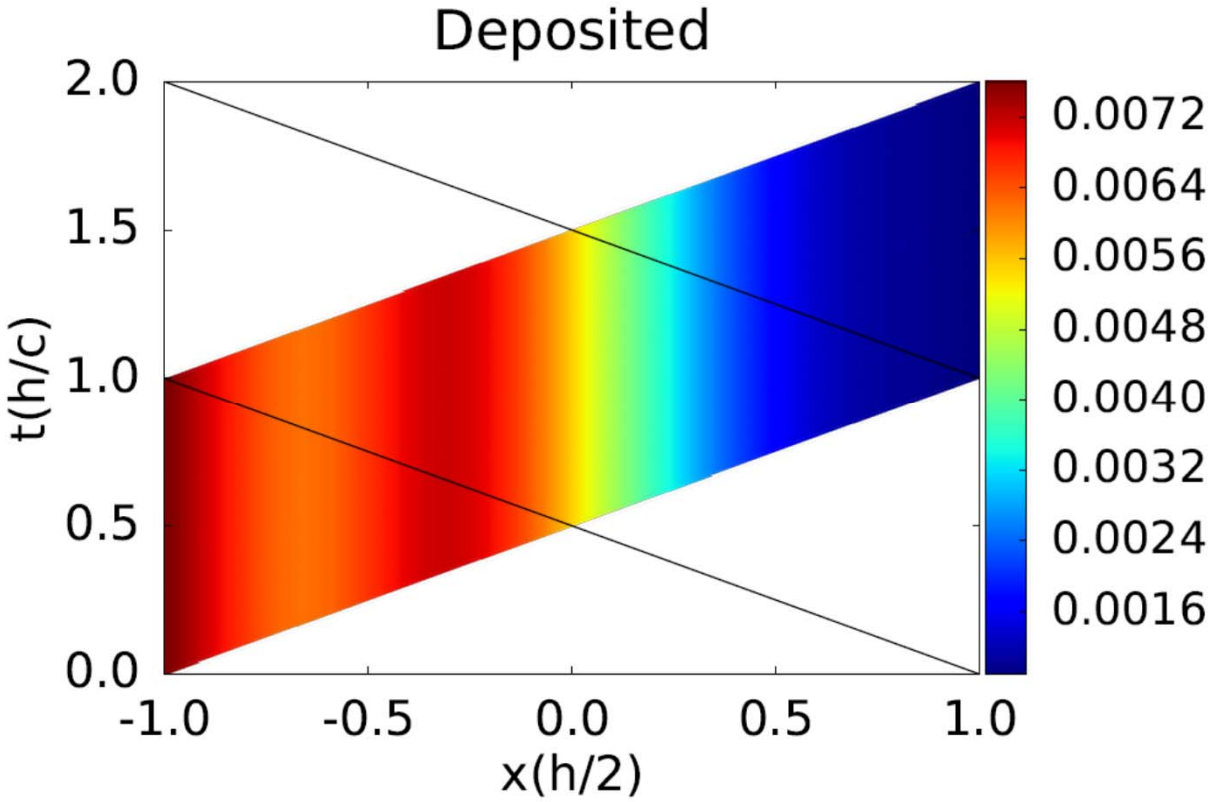

With nano antennas

The absorptivity is increased towards the center, due to the implanted nano antennas.

The deposited energy from laser irradiation from one side only. The absorption is modified by nano antennas so that the absorptivity is increasing towards the middle, so that the deposited energy is constant up to the middle. Then the absorptivity is decreasing, but hardly any energy is left in the irradiation front. Thus again only a negligibly small energy reaches the opposite end of the target.

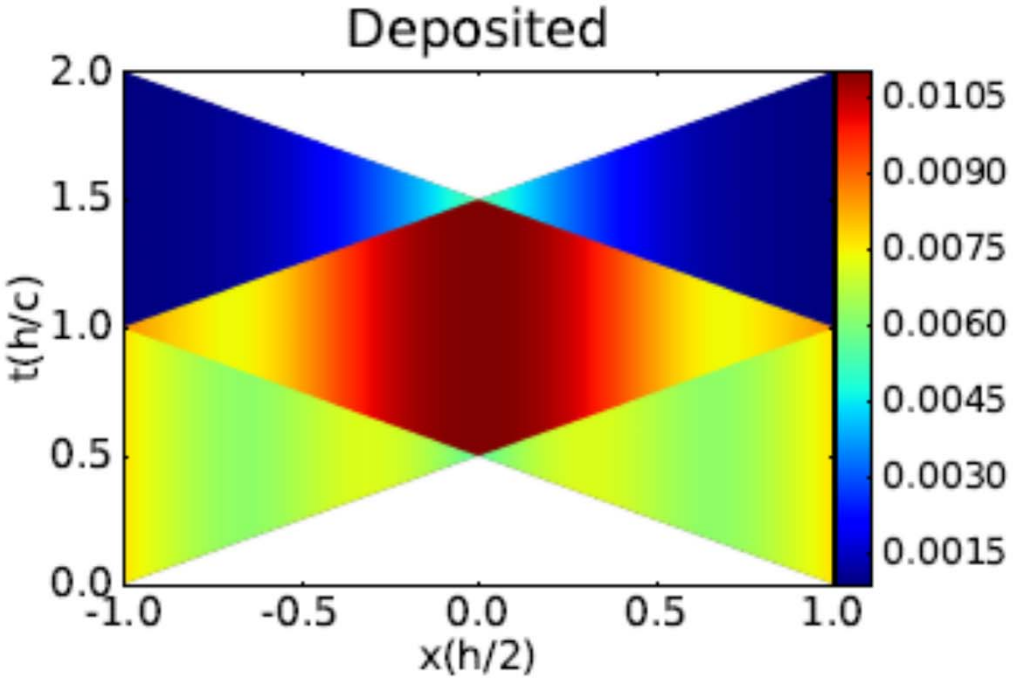

Figure 2: (color online) Deposited energy per unit time in the space-time across the depth, h, of the flat target. The time is measured in units of (h/c), where c is the speed of light in the material of the target. The irradiation lasts for a period of $\Delta t = h/c$ the time needed to cross the target. The irradiated energy during this time period is Q from one side, so it is $2Q$ from both sides together.
The color code indicates the deposited energy per unit time and unit cross section (a.u.). The deposited length is $\Delta x = c\Delta t$. Note! The absorptivity in this case $\alpha_K \neq$ const. For more details please see Appendix B.

With nano antennas

Irradiation from both sides.

Ignition energy is: Q_i/m
e.g. for DT target: $Q_i/m = 27$ kJ/mg
➔ if we have $Q = 100$ J , then
we can have a target mass:
$m_{DT} = Q / Q_i = 0.481$ μg.

Then with m_{DT} and ρ_{DT} given
we get the DT-target's volume, V_{DT}
and $h_{DT} = 0.140$ mm .

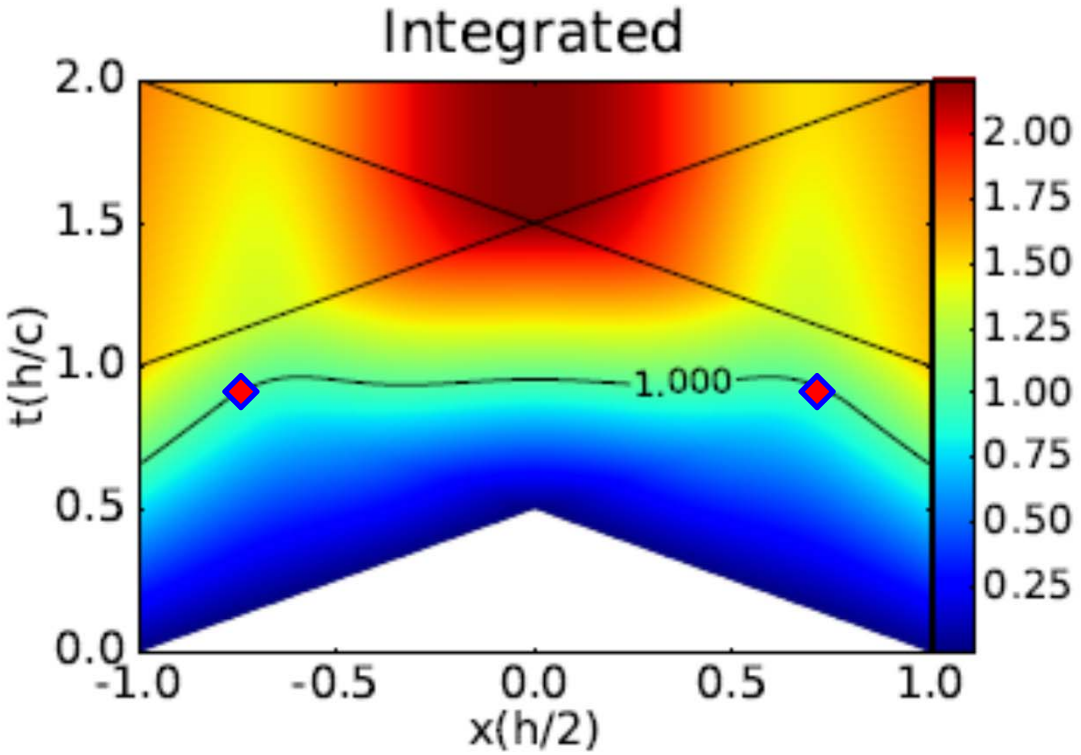

Figure 3: (color online) Integrated energy up to a given time in the space-time across the depth, h, of the flat target. The color code indicates the temperature, T, reached in a given space-time point, in units of the critical temperature, (T_c). The contour line $T = 1$, indicates the critical temperature, T_c where the phase transition or the ignition in the target is reached. This contour line is almost at a constant time, indicating simultaneous whole volume transition or ignition. The irradiated energy, Q is chosen so that, $1Q$ irradiation will achieve the critical temperature.

With nano antennas

Ignition is reached at contour line $Q = 1$.

[L. P. Csernai, M. Csete, I. N. Mishustin, A. Motornenko, I. Papp, L. M. Satarov, H. Stöcker, N. Kroo, ***arXiv***:1903.10896, ***Submitted to MRE***]

Test of principles with smaller pulse energy

1 Relativistic time-like (simultaneous) ignition
2 Using nano antennas to reach whole volume uniform ignition or transition
3 Using 1D geometry, with two beams from opposite direction for realizability

Let us take
a $P = 30\ \mathrm{mJ}$, $1\ \mathrm{ps}$ laser,
a polilactic acid (PLA) target with T = 150 C melting temperature, $Q_i/m = 28\ \mathrm{J/g}$
this leads to $m_i = 1.07\ \mathrm{mg}$ target mass, and $h_i = 1.016\ \mathrm{mm}$ target thickness.

The melting transition profile can be checked by simple and affordable analysis by microscope.

The distribution, and absorption properties of implanted nano antennas can be well optimized.


European Laser
Infrastructure
ELI-ALPS
Szeged, HU

European Laser Infrastructure – Szeged, HU

ELI-ALPS Szeged:
EU Extr. Light Infrastructure
Attosec. Light Pulse Source

2PW High Field laser
10 Hz, <10fs, **20 J**

HAS Wigner RCP, Budapest

Ti-Si Hidra L. 30mJ 10Hz 40fs

Gagik P. Dzsotjan, József Bakos, Gábor Demeter,
Dávid Dzsotjan, Miklós Kedves, Béla Ráczkevi,
Zsuzsanna Sörlei, Péter Lévai

Laser wake acceleration of protons for radiation therapy

- proton beam energy is deposited at a location of a certain depth [Bragg peak]
- tumor treatment with minimal side damage (compared to other radiation therapies)
- target is low density (~ like water or more)
- Collaboration with Peking University, China

These features are similar to the needs of laser induced ICF with nano-plasmonics!
Deposition at a depth via the Bragg peak is an alternative way to get volume ignition

Gábor Veres, István B. Földes, Márk Aladi, Imre Ferenc Barna, Róbert Bolla,
Zsolt Kovács, Mihály Pocsai, Dániel Dunai, Gábor Anda et al.

Fusion plasma diagnostics, ITER, JET etc.

Péter Dombi, Péter Rácz, Norbert Kroo et al.

Laser induced nano-plasmonics

HAS Centre for Energy Research, Budapest
Inst. for Technical Physics and Materials Science

András Deák, S. Pothorsky, D. Zámbó, D. Szekrényes, Z. Hajnal, Béla Pácz et al.

Nano-particle assembly at the single particle level

- manufacturing of Au nano-shells and nano-rods
- imbedded in different concentrations in carriers
- polarized target constructions with nano-rods (for polarized laser irradiation)
- testing resonant light absorption

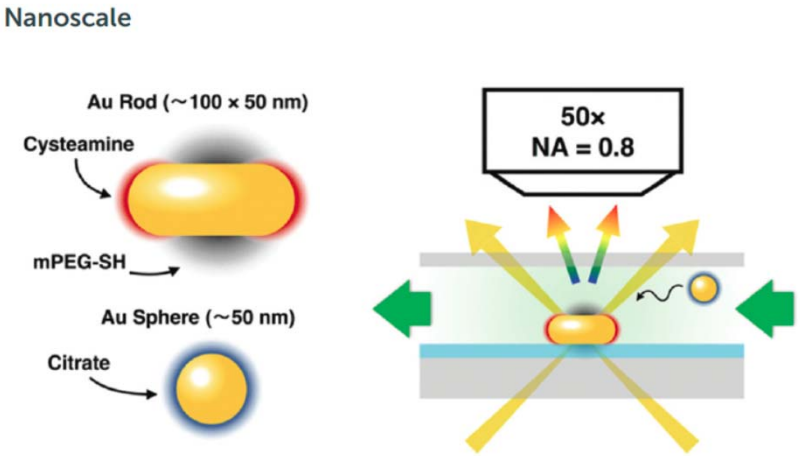

Scheme 1 Schematics of the prepared nanoparticles (left) and the measurement arrangement (right). The patchy nanorods are first immobilized on ITO covered substrates, then the aqueous nanosphere solution is introduced and changes in the scattered spectrum upon binding detected.

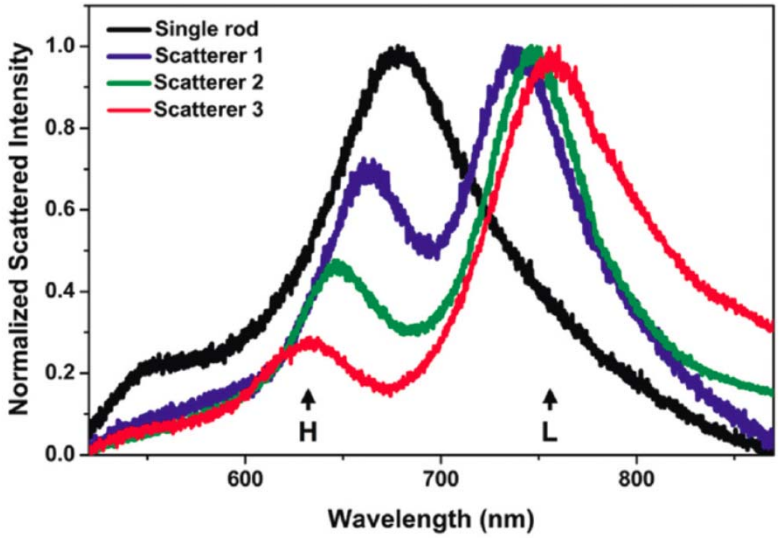

Fig. 1 Typical scattering spectra measured *in situ* in the liquid cell. The appearance of the high (*H*) and low (*L*) energy peaks surrounding the dip indicate the formation of a heterodimer. The spectrum of a single nanorod before the assembly is shown for reference.

[Detecting patchy nanoparticle assembly at the single-particle level, S.Pothorszky et al., Nanoscale 9(2017)10344]

Nano-particle absorption

The target absorptivity is increased via core-shell type plasmonic nano-shells. Calculations via solving the Maxwell equations, and evaluating the ohmic heating were performed.

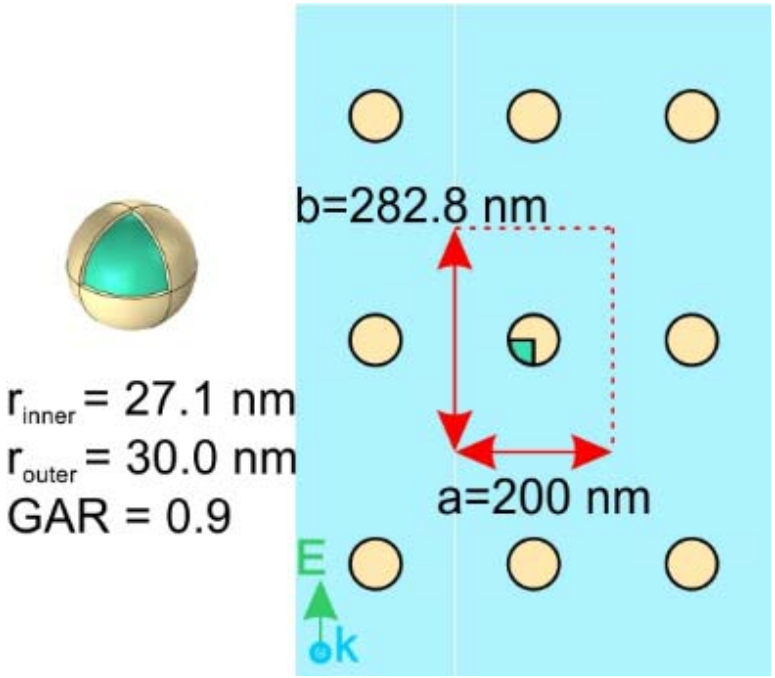

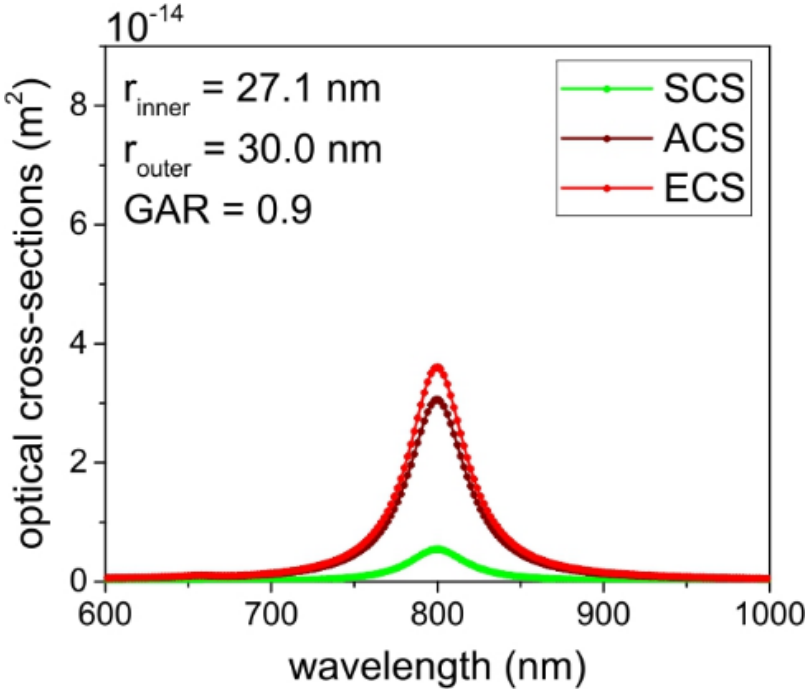

1 ps laser pulse length, λ = 800 nm, One-sided & two-sided irradiation tested, 85-100 % absorption in the target length h. Nano-antenna shapes, layer configurations, layer distribution varied & analyzed.

[M. Csete, et al., University of Szeged, HU]

50 Jahre GSI

FAIR

Bei GSI entsteht das neue Beschleunigerzentrum FAIR.
Erfahren Sie mehr.

GSI ist Mitglied bei

Laser Parameter: PHELIX

	Langer Puls	Kurzer Puls
Pulslänge:	1 - 10 ns	0.5 - 20 ps
Energie:	0.3 - 1 kJ	bis 200 J
Max. Intensität:	10^{16} W/cm^2	2 10^{21} W/cm^2
Kontrast:	50 dB	bis 120 dB

Wissenschaftliche Veröffentlichungen

PHELIX wird genutzt, um verschiedene wissenschaftliche Gebiete, meist in der Plasma- und Atomphysik, zu erforschen. Auf der Seite mit den PHELIX Publikationen, erhalten Sie zusätzliche Informationen, sowie die aktuellsten wissenschaftlichen Veröffentlichungen, die mit den Daten aus Experimenten mit dem PHELIX-Laser erarbeitet wurden.

https://www.gsi.de/work/forschung/appamml/plasmaphysikphelix/phelix.htm

Available resources:

	Pulse energy	Pulse frequency	Pulse length
LLNL NIF 192 laser 3D (1 laser:	11.2 kJ	1/day	~ 10-30 ns
ELI-APLS 2PW High field laser	20 J (34 J)	10 Hz	< 10 fs
BELLA, L. Berkeley Nat. Lab.	34 J	1 Hz	< 30 fs
GSI/FAIR PHELIX laser	200 J	1/90min	> 0.5 ps
Wigner - Coherent Ti-Si Hidra L.	30 mJ (upto 100 mJ)	10 Hz	40 fs
Optimal for laser induced ICF with nano-plasmonics tests	~ 100 J	1 Hz	1-10 ps !

Experimental test of similar configuration @ ShenGuang-II Up, Shanghai :

Nuclear probes of an out-of-equilibrium plasma at the highest compression

Phys. Lett. A 383 (2019) 2285-2289.

G. Zhang [a,b,*], M. Huang [c], A. Bonasera [d,e,*], Y.G. Ma [f,b,i,*], B.F. Shen [g,h,*], H.W. Wang [a,b], W.P. Wang [g], J.C. Xu [g], G.T. Fan [a,b], H.J. Fu [b], H. Xue [b], H. Zheng [j], L.X. Liu [a,b], S. Zhang [c], W.J. Li [b], X.G. Cao [a,b], X.G. Deng [b], X.Y. Li [b], Y.C. Liu [b], Y. Yu [g], Y. Zhang [b], C.B. Fu [k], X.P. Zhang [k]

4 (up) + 4(down) lasers
Target thickness, h (3.6μm-1mm) & radius, R, (150-400μm) were varied.

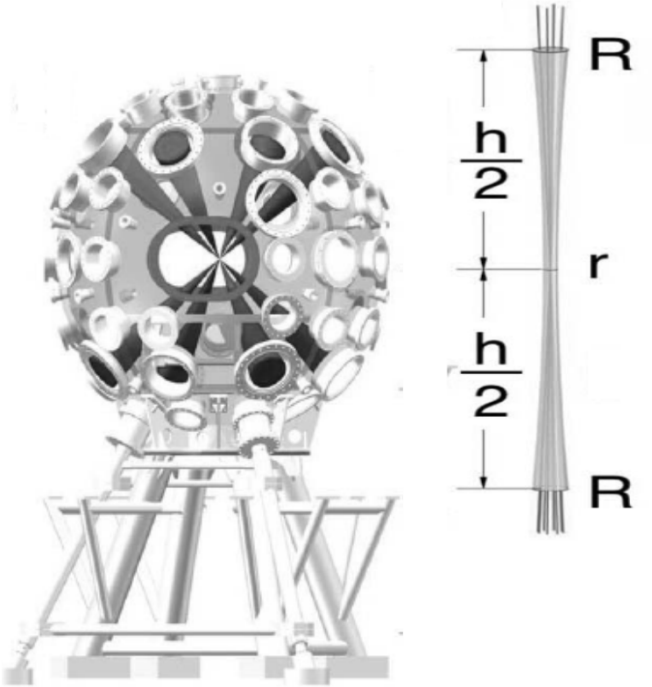

Total pulse energy 1.2kJ (2ns) for 8 beams.
Shortest (250ps) pulses -> 100s MeV ions > non-thermal distr. = directed ion acceleration

Typical fusion neutron energies were measured & used to extract the target density.

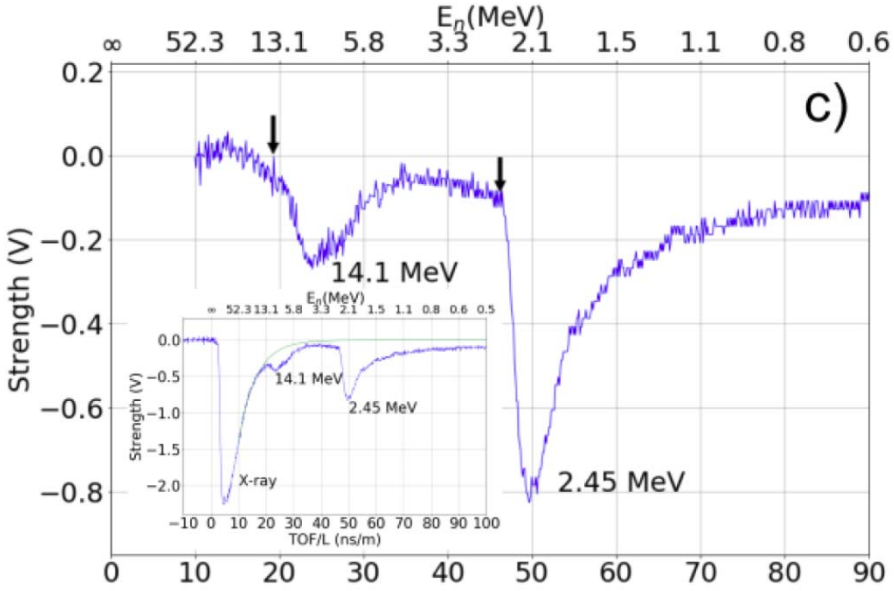

Experimental test of similar configuration @ ShenGuang-II Up, Shanghai :

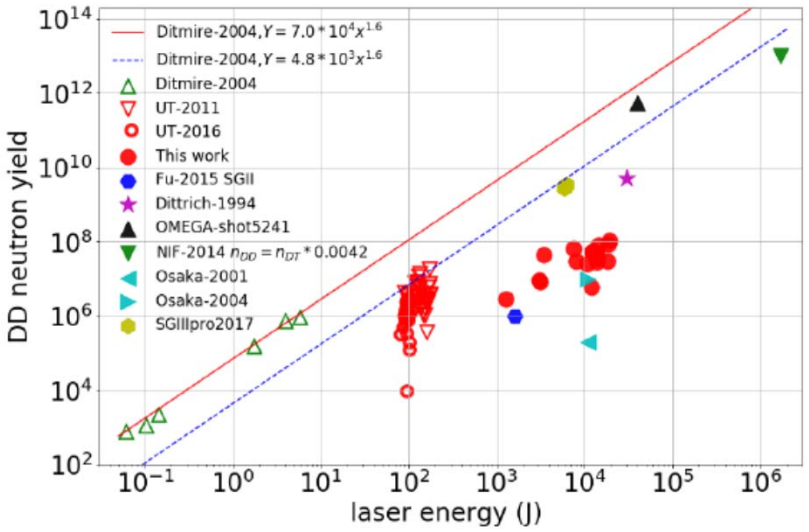

Figure 3: (color online) Fusion yield as function of laser energy. Different experimental results Ditmire-2004[40], UT-2011[20], UT-2016[19], Fu-2015 SGII[45], Dittrich-1994[49] , NIF-2014[48] , Osaka -2001[46], Osaka-2004[47], OMEGA-shot5241[41]and SGIIIpro2017[42] are indicated in the inset.

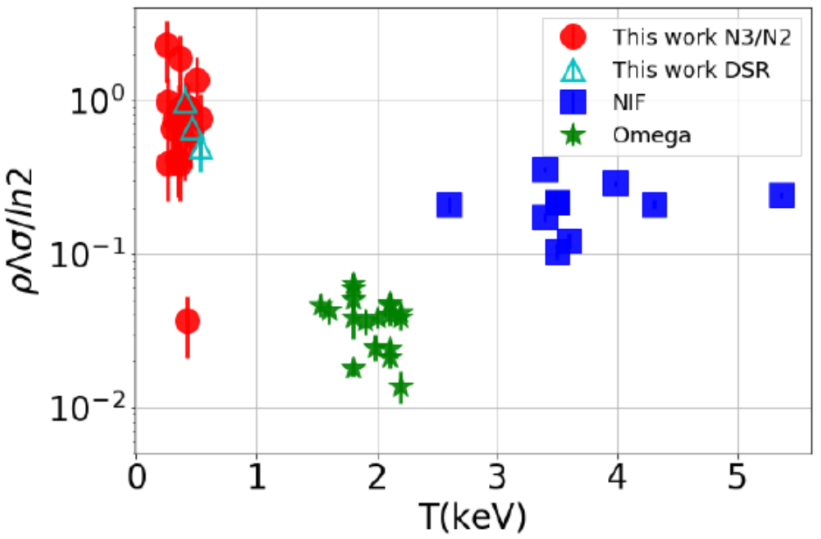

Figure 4: (color online) $\Lambda\rho\sigma/\ln 2$ obtained from eq.(4) vs T from eq.(1). Omega and NIF data are derived from the experiments[25], using the Down Scatter Ratio[23, 21]. Our results using the DSR method (N_4/N_3) are given by the open triangle symbols in good agreement with the N_3/N_2 ratios.

Stimulated by these considerations we decided not to fight non-equilibrium effects but rather enhance them, i.e. study plasmas highly compressed and completely out of equilibrium.

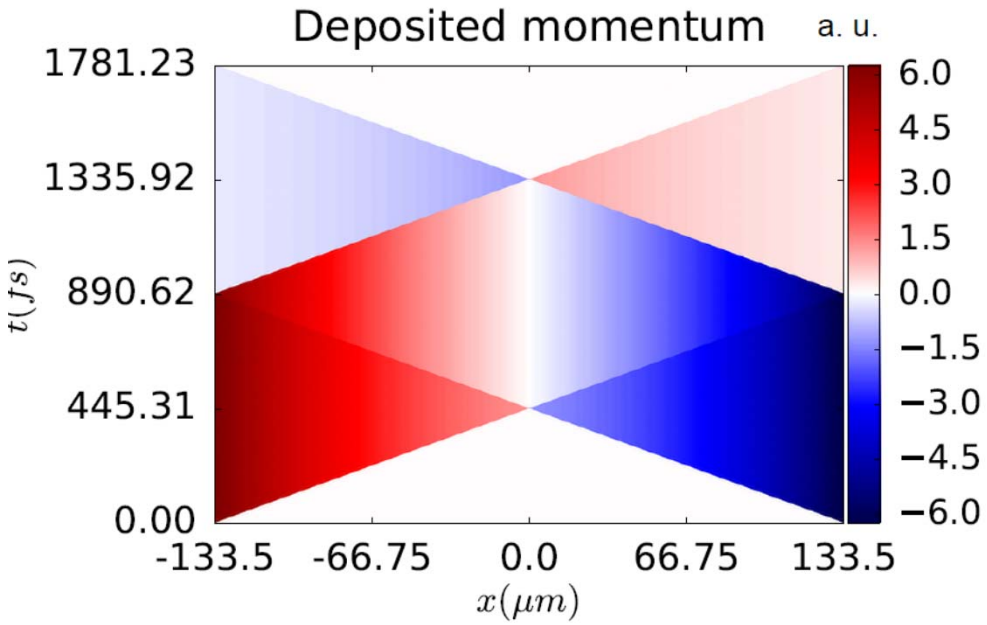

Deposited momentum

Leads to compression w/o external ablator surface
[Gyulassy, Csernai, NPA 1986]
→ **leads to QGP formation w/o RT instabilities**

Implanted nano-antennas increase further the compression !!

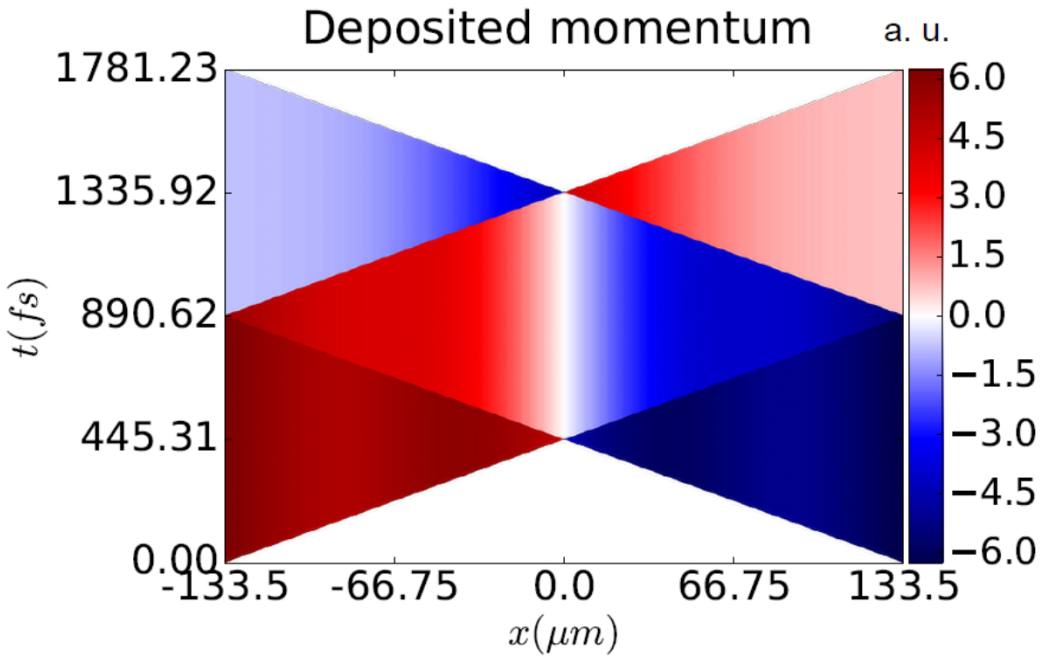

LLNL – NIF April 2019

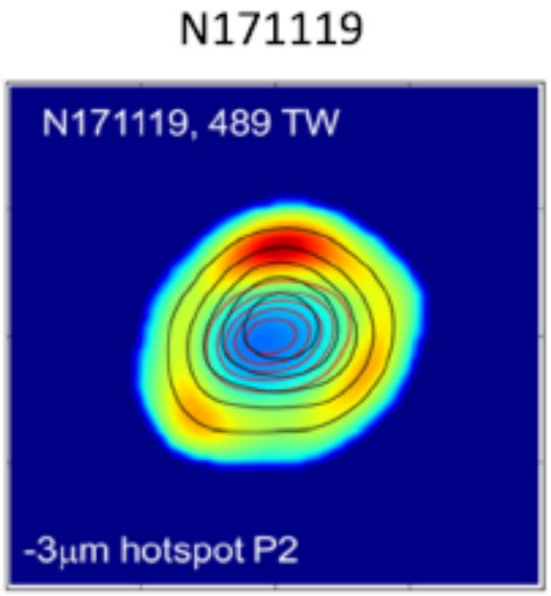

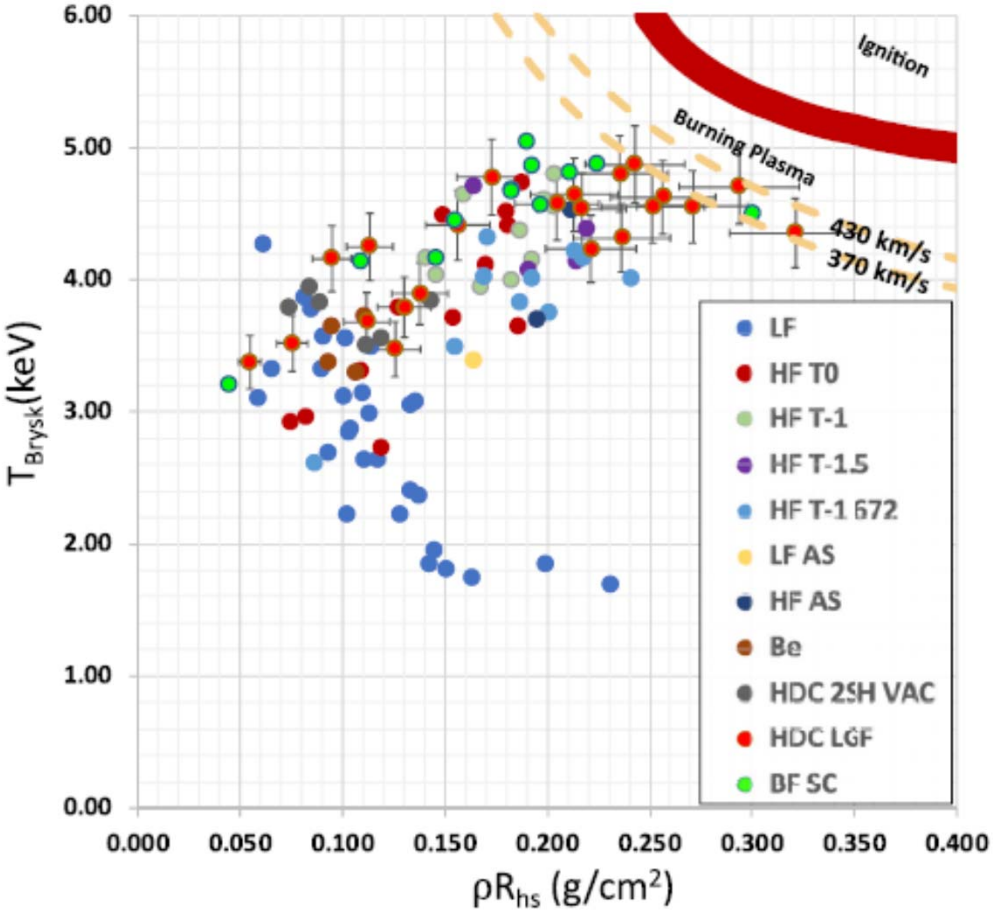

Hot-spot, 3μm, burning spreads by α-heating: boundary is approached.

[O.A. Hurricane et al., Phys. Plasmas 26, 052704 (2019) April.]

Thus, ultra-relativistic heavy ion physics lead to discovery Quark Gluon Plasma (QGP), but also to advances in
(i) relativistic fluid dynamics (RFD).

With **(ii)** nano technology this may revolutionize in a simple, and **(iii)** affordable 1D geometry the technological development of
(➔ iv) Inertial Confinement Fusion.

This methodology may be used to study other dynamical, radiation dominated processes.

*

Laser Wake Field Acceleration

http://www2.mpq.mpg.de/lpg/research/LWFA/LWFA.html

Case I : The highly non-linear broken-wave regime

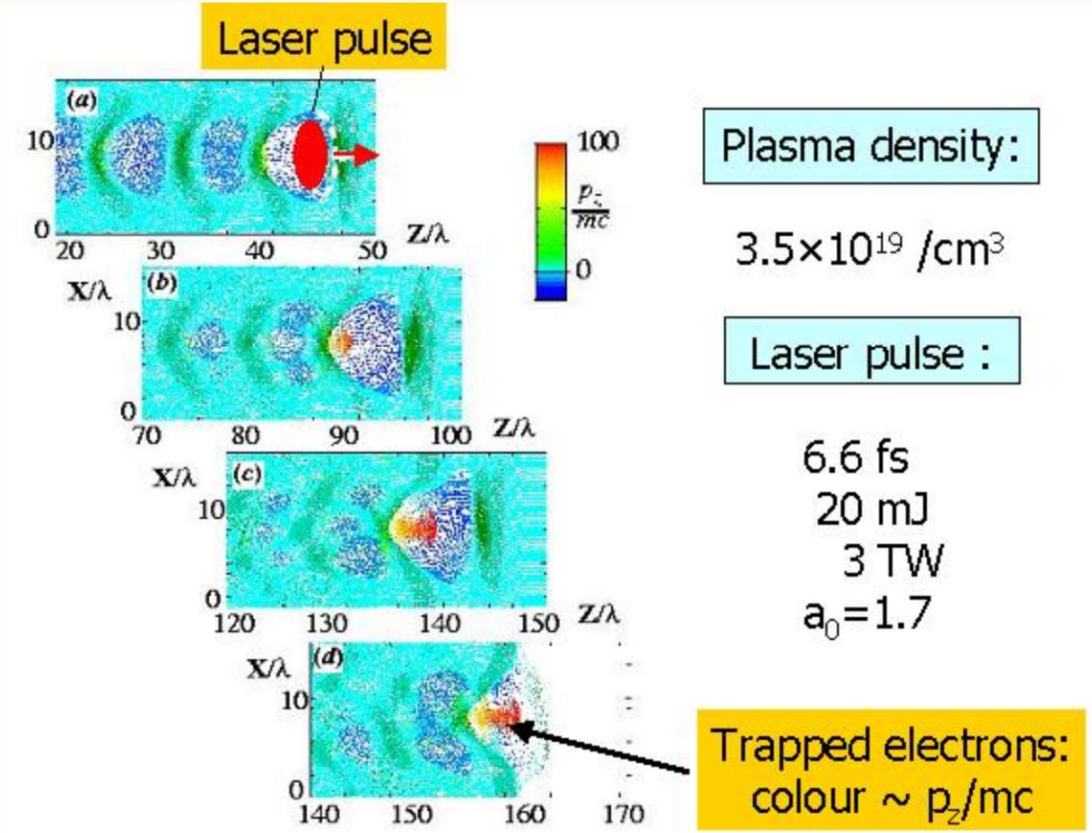

Here we show the wakefield evolution of a 20 mJ, 6.6 fs laser pulse, simulated with the 3D-PIC code VLPL. Electron density is plotted in four frames (snapshots at different times) with colour representing p_z/mc. A typical plasma wave is seen trailing the laser pulse with green wave crests moving to the right and low-density plasma in between moving to the left. In frame (a) the laser pulse is also shown explicitly and is seen to fit into the first wave bucket. A prominent feature is the red stem of high-energy electrons growing out of the rear vertex of the the first wave bucket. These electrons originate from wavebreaking which occurs at this vertex first and spills electrons into the wave trough where they are strongly accelerated by the electric field in the wake. When the wave arrives at the rear side of the thin plasma layer, this wave trough opens and releases a bunch of relativistic electrons which is just a few μm long. You may look at this process in more detail in the movie:

A. Pukhov and J. Meyer-ter-Vehn, Appl. Phys. B74, 355 (2002)

Case II : The solitary bubble regime

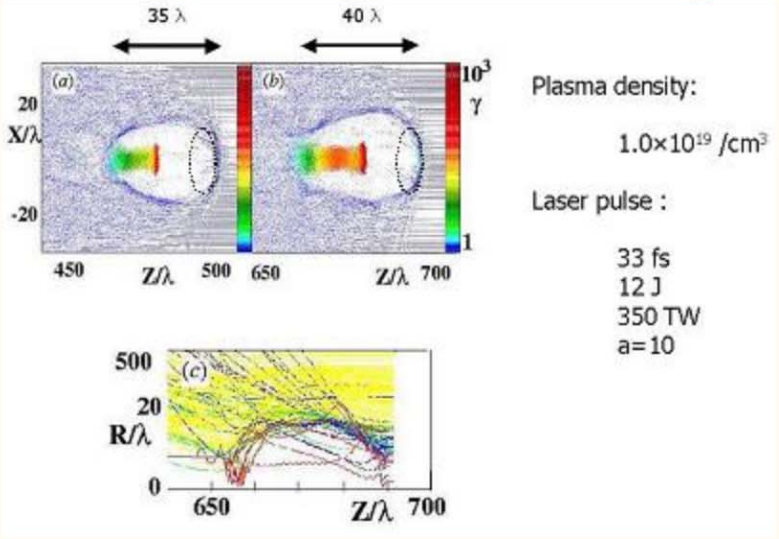

In this second case, a laser intensity significantly above the wave-breaking limit ($a=eA/mc^2=10$) has been chosen such that the wakefield breaks completely after the first oscillation and only a single wakefield bubble survives which is practically void of electrons. Part (c) of the figure below shows electron trajectories in a comoving frame. Yellow electrons are only slightly perturbed by the laser pulse, blue electrons are scattered away, while red electrons hit by the central part of the laser pulse form the mantle of the bubble and are predominantly trapped in the bubble. The trapping is so efficient that after a certain propagation distance there are more trapped electrons in the bubble than were initially in the same volume. At this point beam-loading effects set in and the bubble starts to stretch; after 500 laser cycles the extension is 35 λ and after 700 laser cycles 40 λ. This stretching has a significant effect on the energy spectrum.

Generation of relativistic ions

D. Habs, G. Pretzler, A. Pukhov and J. Meyer-ter-Vehn, Progress in Particle and Nuclear Physics 46, 375 (2001).

1 kJ, 15 fs pulses incident on 30 μm plastic foil may result in 10^{14}, 4-5 GeV protons.

1 kJ , 15 fs laser pulse
focussed on 10 μm spot
of $10^{22}/cm^3$ plasma

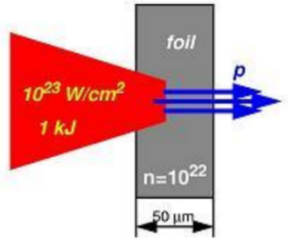

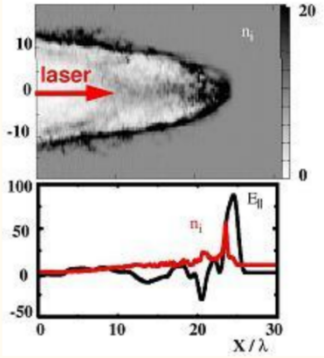

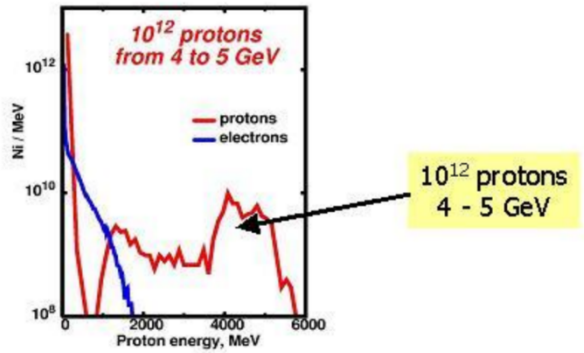

Target size ➔ required ignition pulse length for simultaneous (time-like) ignition

Target thickness 2L [m]		Max Pulse time 3L/c [s]	
2.00E-03	mm	1.00E-11	10 ps
2.00E-04	100 µm	1.00E-12	ps
2.00E-05	10 µm	1.00E-13	100 fs
2.00E-06	µm	1.00E-14	10 fs
2.00E-07	100 nm	1.00E-15	fs
2.00E-08	10 nm	1.00E-16	100 as
2.00E-09	nm	1.00E-17	10 as

Another Option to Reach Volume Ignition
Heavy-Ion Beams – FAIR & NICA

- Energy deposition by heavy ion beams – Bragg peak!
- Absorption depth can be tuned! ➔
- Beam bunch energy distribution could be achieved
- Present Bunch length is ~ 70 ns
- Bunch length of 10 ps may be reached [B. Sharkov]
- ➔ **Proposal(s), Patent(s), Laser wake acc. ?**

Time-like detonation in presence of magnetic field

Ritam Mallick* and Shailendra Singh
Indian Institute of Science Education and Research Bhopal, Bhopal, India
(Dated: August 6, 2018)

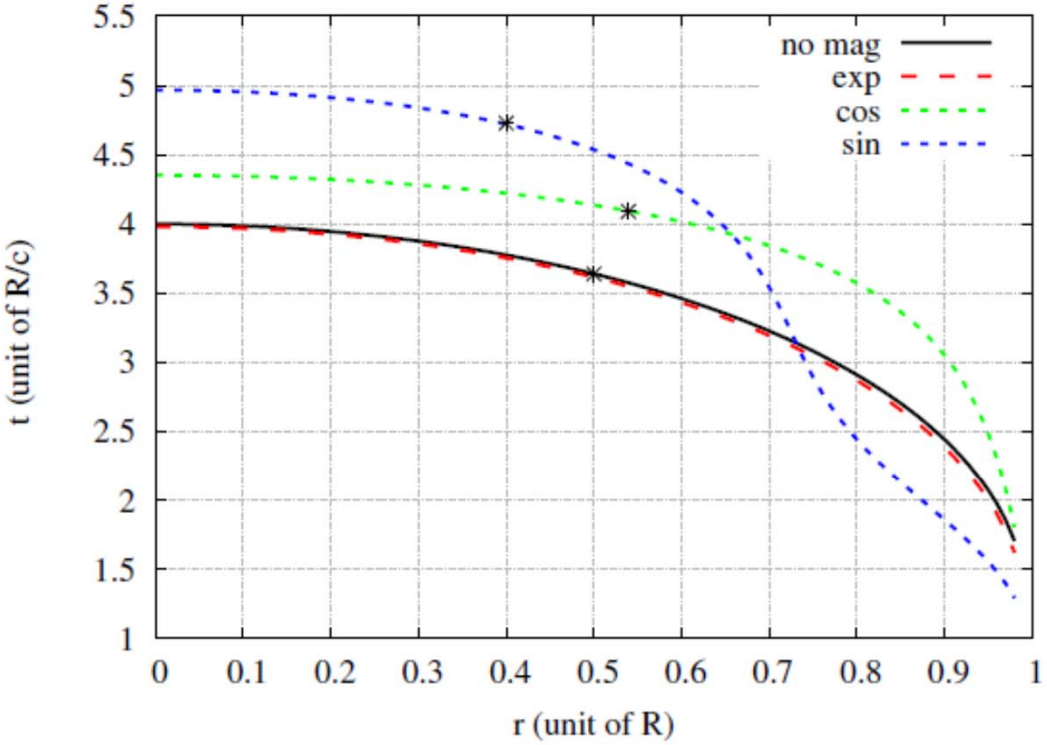

FIG. 1. Contour $T(r,t) = T_c$ for non magnetic and magnetic curves are drawn. The values of the normalized parameters are $K = 1 = \frac{4\pi CQ}{C_v}$, $\alpha = 1.0$ and $T = 3$ (in unit of $\frac{2\pi CQ}{C_v}$).

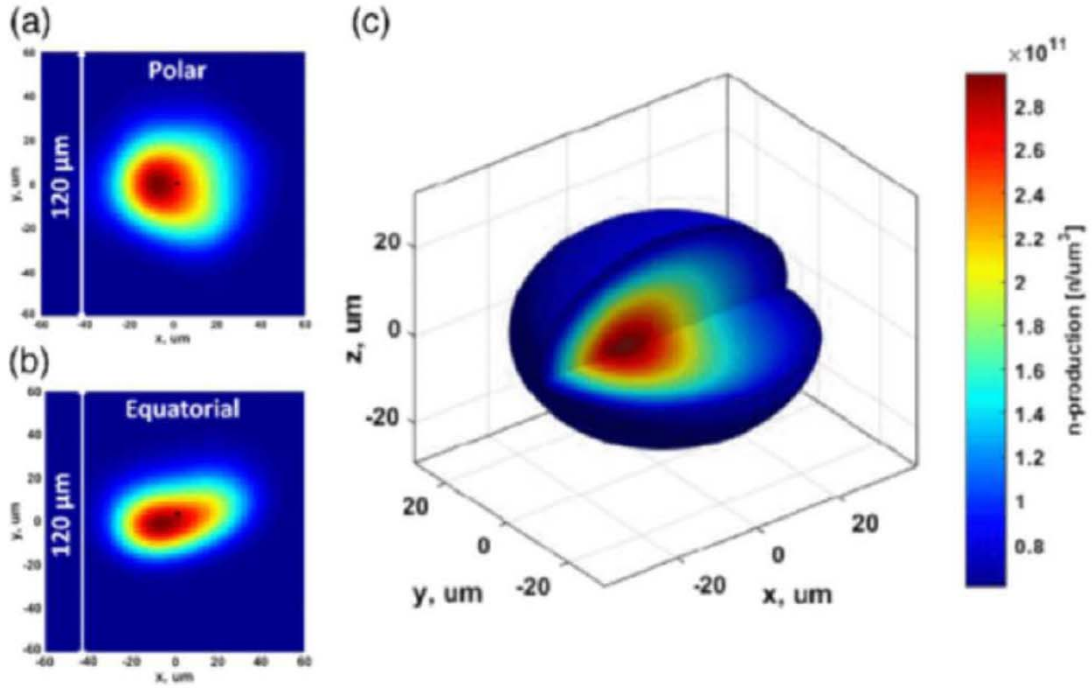

Figure 3

Shot N170601. (a) Polar neutron image. (b) Equatorial neutron image. (c) Three-dimensional reconstructed neutron volume of the hot spot.

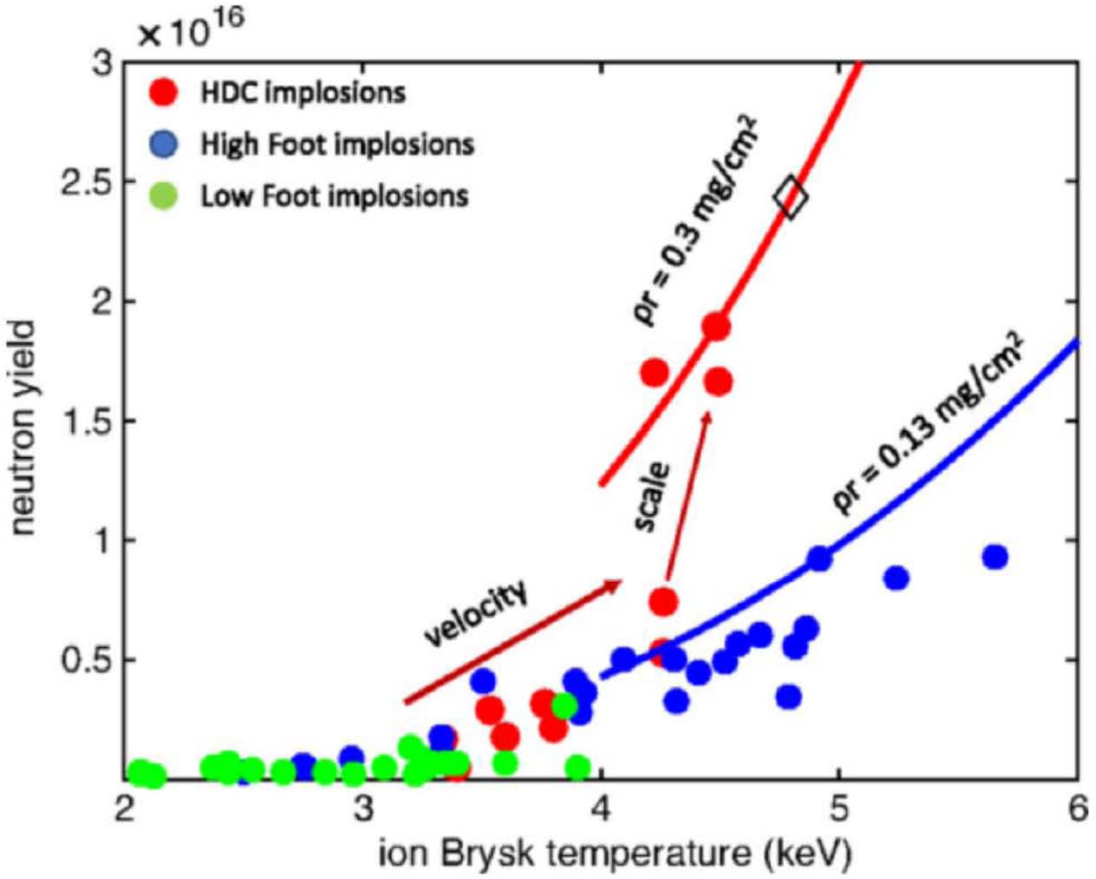

Figure 4

Total DT neutron yield as a function of ion temperature, red dots are doped HDC implosions, blue dots are high foot implosions, green dots are low foot implosions. The neutron yield is plotted against the lowest burn averaged DT ion temperature measured by NTOF detectors (Brysk temperature). For high foot implosions, the Brysk temperature is estimated to be up to a keV higher due to flows in the hot spot. Black diamond is the point where α deposited energy equals bremsstrahlung and conduction losses. Solid curves are a yield extrapolation with temperature using a constant ρr and adiabat.